

2 to  $3 \cdot 10^{-41}$ . The fundamental frequency of the vibration is for the initial states about  $6400 \text{ cm.}^{-1}$ ; for the end states, among which the normal state is probably found, about  $5000 \text{ cm.}^{-1}$ .

In conclusion the author wishes to express his thanks to Prof. N. Bohr for his constant help and advice during the work.

---

*On the Interpretation of X-Ray, Single Crystal, Rotation Photographs.*

By J. D. BERNAL, B.A.

(Communicated by Sir William Bragg, F.R.S.—Received July 24, 1926.)

In the development of the study of crystals by X-rays the methods used divide themselves naturally into four types: the Bragg Ionisation Spectrometer method, the Laue method, the Powder method of Debye and Scherrer, and the Rotating Crystal method of Rinne, Schiebold and Polanyi. The techniques of the first three of these methods are fully explained in such books as 'X-Rays and Crystal Structure,' by W. H. and W. L. Bragg, 'The Structure of Crystals,' by Wyckoff, and 'Krystalle und Rontgenstrahlen,' by Ewald, as well as in original papers. On the other hand, the rotation method is only slightly touched on in these works, the literature is scattered in a great number of papers, and the technique has not so far been described at any length in a convenient form. Particularly in English, references to it are scanty.

In this paper the author has tried to give a concise account of the method, together with various types of charts and tables as it is used in the Davy Faraday Laboratory. The methods described differ in certain respects from those used on the Continent,\* but they have been found to be rapid and sufficiently accurate.

In the rotation method proper a small crystal, mounted on a spindle which can be revolved at a uniform speed, is rotated in front of a narrow beam of homogeneous X-rays and the beams of X-rays reflected record themselves as spots on a plate or film placed behind the crystal. In the more developed form of the oscillation method, instead of a complete rotation, the spindle is turned backwards and forwards at a constant speed through some definite small angle. It is not within the scope of the present paper to describe the forms of apparatus which may be used for this purpose; they will be touched

\* For a convenient summary, see Schiebold, 'Z. f. Physik,' vol. 28, p. 355 (1924).

on only in so far as they have a bearing on the mathematical interpretation of the experimental results.

In the analysis of crystal structures by any of the methods so far used, the experimental data are all comprised in the knowledge of the intensities of the X-ray reflections from every one of the triply infinite series of crystallographic planes in a crystal. Naturally in practice it is only a question of measuring as many of these reflections as possible, especially those of small crystallographic indices. The procedure can be conveniently divided into three stages :—

- (i) the determination of the size and shape of the unit cell of the fundamental lattice of the crystal ;
- (ii) the determination of the indices of the reflecting planes leading to the determination of the space group ;
- (iii) the measurement of the intensity of the reflection from each plane leading to the complete determination of the structure.

The rotation method is best suited to the first two of these stages, and though its use is being extended to the last, only the first two will be dealt with here.

The understanding of the phenomena of crystal diffraction of X-rays is much helped by a consideration of the reciprocal lattice. This conception was first used by Ewald,\* to whose paper reference should be made, but the account given here refers more particularly to the rotation method and to graphical applications.

We may consider the crystal in the first place as a simple space lattice. Choosing one point of the lattice as origin, we may take the three vectors  $a$ ,  $b$ ,  $c$ , as three primitive translations which form a primitive triplet. Any plane of this lattice may be represented by the indices  $h$ ,  $k$ ,  $l$ , where the intercepts of such a plane on  $a$ ,  $b$ ,  $c$ , are  $a/h$ ,  $b/k$ ,  $c/l$ , respectively. We will, however, restrict the term "plane" to those planes for which  $h$ ,  $k$ ,  $l$ , are integers (not necessarily prime to each other). In other words, in any set of parallel crystallographic planes, we choose the one nearest the origin and the planes parallel to this whose distances from the origin are sub-multiples of its distance from the origin. The former planes are responsible for the first-order X-ray reflections, the latter for the higher orders.

Now, from the planes of the lattice, as so defined, another lattice can be built up each point of which lies on the normal from the origin to a plane and at a distance  $\rho$  from the origin,  $\rho$  and the spacing  $d$  of the plane being related by

$$\rho d = k^2,$$

\* 'Z. f. Kryst.', vol. 56, p. 129 (1921).

where  $k$  is a constant. In other words, each point in the new lattice is the reciprocal polar of a plane in the old lattice in a sphere of radius  $k$ . The new lattice is consequently called the reciprocal lattice of the old. By applying to the new lattice the same operation, we arrive at a replica of the old lattice. For every plane in one there corresponds a point in the other and vice versa (see fig. 1).

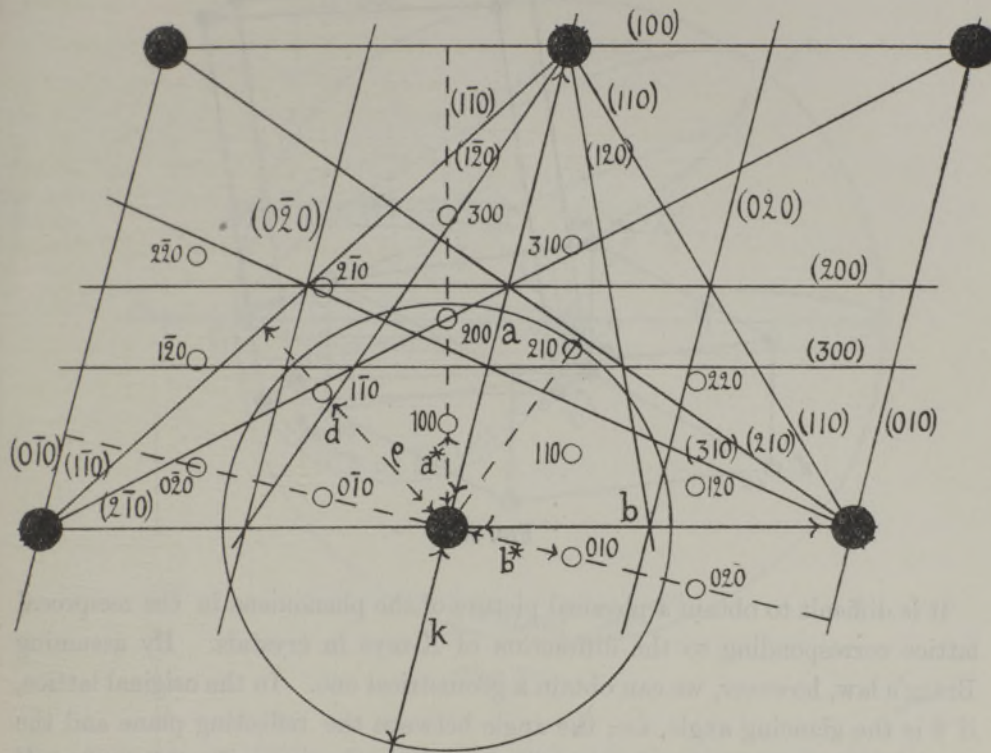


FIG. 1.

● Point of Lattice. (310) Plane of Lattice. ○ 310 Point of Reciprocal Lattice.

We may refer this reciprocal lattice to a set of vectors  $a^*$ ,  $b^*$ ,  $c^*$ , reciprocal to the set  $a$ ,  $b$ ,  $c$ , i.e., such that in general

$$a^* = \frac{k^2 bc}{\Delta} \sin \alpha \text{ and is perpendicular to the plane } bc,$$

$$b^* = \frac{k^2 ca}{\Delta} \sin \beta \text{ and is perpendicular to the plane } ca,$$

$$c^* = \frac{k^2 ab}{\Delta} \sin \gamma \text{ and is perpendicular to the plane } ab,$$

where  $\Delta$  is the volume of the parallelepipedon  $abc$ . A lattice built upon  $a^*$ ,  $b^*$ ,  $c^*$ , as primitive translations will be the reciprocal lattice of that built up on  $a$ ,  $b$ ,  $c$ , and vice versa (see fig. 2). If  $(h, k, l)$  are the indices of any plane in the original lattice, then the corresponding point in the reciprocal lattice has for co-ordinates  $h, k, l$ .

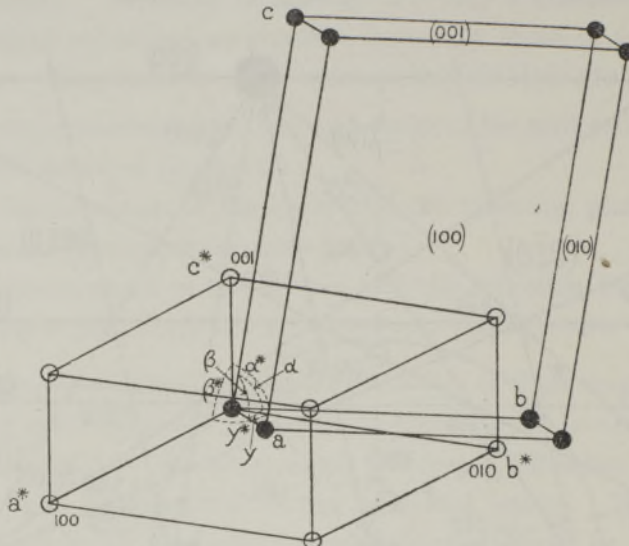


FIG. 2.

It is difficult to obtain a physical picture of the phenomena in the reciprocal lattice corresponding to the diffraction of X-rays in crystals. By assuming Bragg's law, however, we can obtain a geometrical one. In the original lattice, if  $\theta$  is the glancing angle, *i.e.*, the angle between the reflecting plane and the normal to the wave front of the incident beam, reflection only takes place if

$$\sin \theta = \frac{\lambda}{2d}.$$

In the reciprocal lattice the wave fronts reciprocate into points travelling along their normal and  $\theta$  becomes the angle between the incident ray and the plane through the corresponding point in the reciprocal lattice which is normal to its radius vector. As this radius vector  $\rho = k^2/d$  we have as the expression analogous to Bragg's law

$$\sin \theta = \frac{\lambda \rho}{2k^2}.$$

The value of the use of the reciprocal lattice is that as every point in it corresponds to a reflection of a plane in the original crystal, it also corresponds to

a spot on the photograph, and the arrangement of spots on the photograph is similar to the arrangement of points in the reciprocal lattice.

The reflection of X-rays is shown geometrically in fig. 3. If we consider a sphere of radius  $2k^2/\lambda$  cutting the plane PQR, drawn through the point P normal to its radius vector PO, in the circle QR, then the angle OQP satisfies

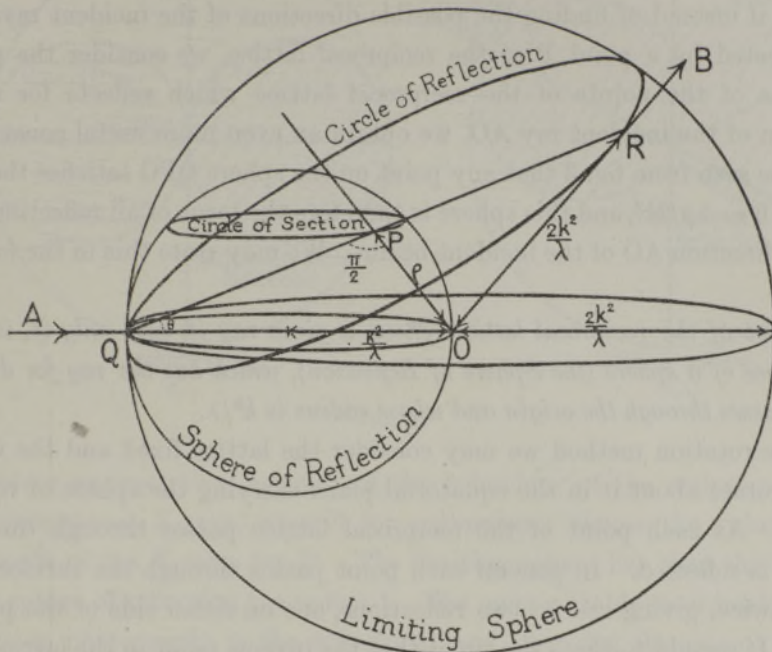


FIG. 3.

the condition  $\sin OQP = \lambda\rho/2k^2$ , and that AO therefore represents a ray direction which will be reflected by the plane in the original lattice corresponding to the point P, or, as we may say in short, that AO is ray reflected by the point P, the reflected ray being OB. Further, all rays that can be reflected by P lie along the cone OQR and the incident and reflected rays are diametrically opposite generators of this cone. Here we have a simple geometrical picture of reflection as it occurs in the reciprocal lattice ; it may be stated as follows :—

*A ray is reflected by a given point of the reciprocal lattice if and only if it lies along a generator of a cone (the Cone of Reflection), whose apex is the origin and whose base is the circle (the Circle of Reflection), which is the intersection of the plane through the point normal to its radius vector, and a sphere (the Limiting Sphere), whose centre is the origin and whose radius is  $2k^2/\lambda$ . The corresponding*

reflected ray is the diametrically opposite generator.. It is obvious that no real cone of reflection can be formed by any point outside the sphere of radius  $2k^2/\lambda$ ; such points, therefore, cannot reflect, and the sphere is accordingly called the *Limiting Sphere*. The number of reflecting points varies as the volume of this sphere and consequently inversely as  $\lambda^3$ . This is an important consideration in choosing wave-lengths.

Now, if instead of finding the possible directions of the incident rays which are reflected by a point P of the reciprocal lattice, we consider the possible positions of the points of the reciprocal lattice which reflects for a given direction of the incident ray AO, we obtain an even more useful construction. It can be seen from fig. 3 that any point on the sphere QPO satisfies the condition  $\sin \theta = \lambda\rho/2k^2$ , and this sphere is therefore the locus of all reflecting points for the direction AO of the incident beam. We may state this in the following form :—

*A point of the reciprocal lattice reflects a given ray if, and only if, it lies on the surface of a sphere (the Sphere of Reflection), which has the ray for diameter, which passes through the origin and whose radius is  $k^2/\lambda$ .*

In the rotation method we may consider the lattice fixed and the incident ray to rotate about it in the equatorial plane carrying the sphere of reflection with it. As each point of the reciprocal lattice passes through the sphere the ray is reflected. In general each point passes through the surface of the sphere twice, giving rise to two reflections, one on either side of the principal plane. If we add to these the times that the inverse point in the lattice passes through the sphere, we have four intersections corresponding to the four symmetrically disposed reflections of a plane in the original lattice. In one complete revolution the sphere of reflection sweeps out a tore. This tore contains all the points which can reflect for any given position of the axis of rotation. If the reflected rays were received on a spherical surface, we should be able to register all the reflections; with the use of plates or cylindrical films we only register those lying in a limited portion of the tore. The sections of the tore registering for plates or films is shown in fig. 4a. It is plain that one rotation photograph will not contain nearly all the reflecting planes, though it will contain the great majority of those near the centre. However, three tores of reflection whose axes are mutually at right angles occupy nearly all the space of the limiting sphere and fill that near the origin at least twice.

In the more general case when the incident ray is not perpendicular to the axis, the surface swept out is a interlacing tore, shown in section in fig. 4b. It can be seen that though each point will still in general intersect the sphere

of reflection four times, the four reflections will now consist of two pairs not symmetrically disposed about the equatorial line.

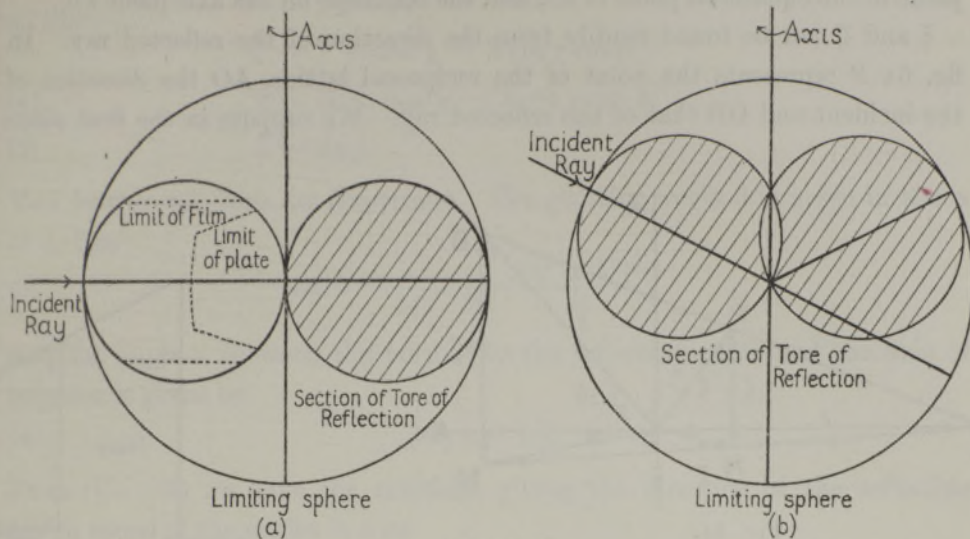


FIG. 4.

To obtain an analytical account of the behaviour of the reciprocal lattice with homogeneous X-rays, we will for convenience choose the value  $\lambda$ , the wave-length of the X-rays, for  $k^2$ . The limiting sphere has then the radius 2 and the sphere of reflection the radius 1. The most suitable co-ordinate system for rotation photographs is the cylindrical, and, choosing the axis of rotation as axis, we designate the co-ordinates of any point of the reciprocal lattice by  $\xi, \zeta, \omega$  (corresponding to the usual  $u, z, \phi$ ). As long as we are dealing with complete rotations the angular co-ordinate  $\omega$  is indeterminate, and for the moment

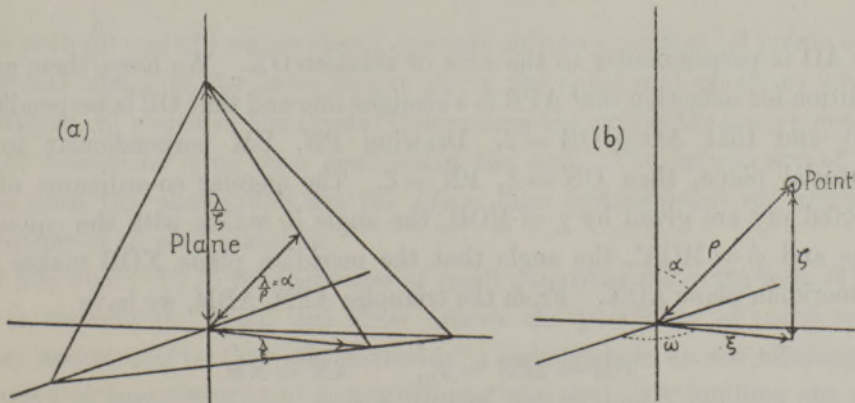


FIG. 5.

we will leave it out. Considering  $\xi$  and  $\zeta$  in terms of the original lattice, we see from fig. 5 that the distance from the origin to the trace of the corresponding plane in the equatorial plane is  $\lambda/\xi$  and the intercept on the axis itself  $\lambda/\zeta$ .

$\xi$  and  $\zeta$  can be found readily from the direction of the reflected ray. In fig. 6A P represents the point of the reciprocal lattice, AO the direction of the incident and OB that of the reflected ray. We suppose in the first place

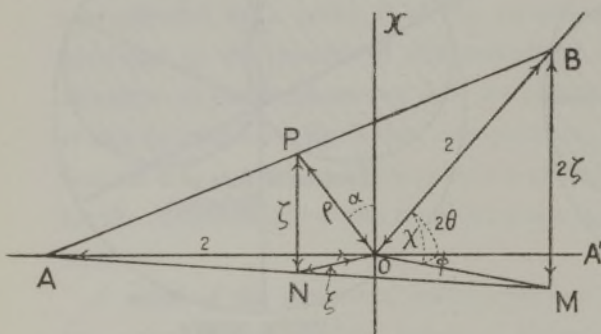


FIG. 6A.

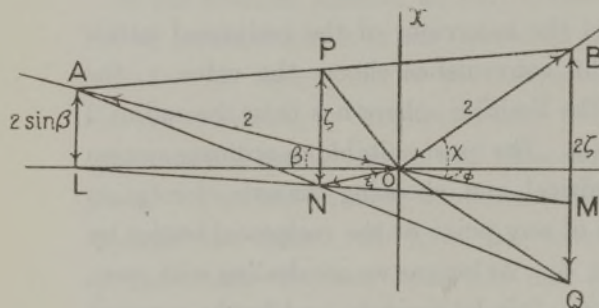


FIG. 6B.

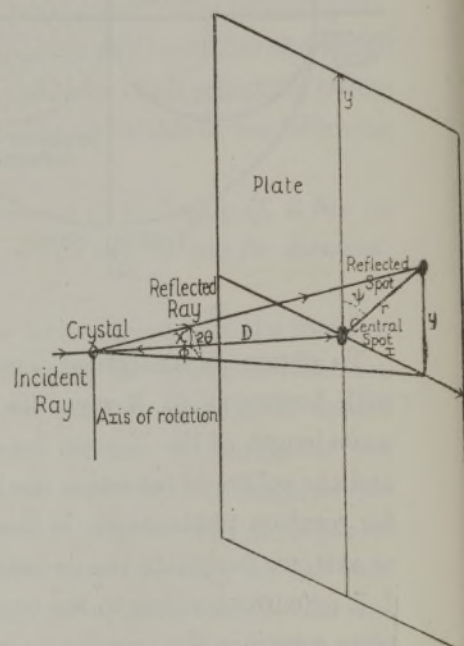


FIG. 7.

that AO is perpendicular to the axis of rotation OX. We have, then, as the condition for reflection that APB is a straight line and that OP is perpendicular to it and that  $AO = OB = 2$ . Drawing PN, BM perpendicular to the equatorial plane, then  $ON = \xi$ ,  $PN = \zeta$ . The angular co-ordinates of the reflected ray are given by  $\chi = MOB$ , the angle it makes with the equatorial plane and  $\phi = MOA'$ , the angle that the meridian plane XOB makes with the meridian plane AOX. From the triangles APN, ABM, we have

$$BM = 2PN = 2\zeta, \quad AN = NM,$$

$$\sin \chi = \zeta, \quad OM = 2 \cos \chi.$$

From the triangle AOM in which ON bisects AM

$$4 \cdot ON^2 = AO^2 + OM^2 - 2 \cdot AO \cdot OM \cos \phi,$$

so that

$$\xi^2 = 1 + \cos^2 \chi - 2 \cos \chi \cos \phi,$$

$$(1) \quad \xi = \{1 + \cos^2 \chi - 2 \cos \chi \cos \phi\}^{\frac{1}{2}},$$

$$(2) \quad \zeta = \sin \chi.$$

Two further relations are important. The glancing angle  $\theta$  is given in terms of  $\xi, \zeta$  as

$$(3) \quad \sin \theta = \frac{\lambda}{2d} = \frac{\rho}{2} = \frac{\{\xi^2 + \zeta^2\}^{\frac{1}{2}}}{2},$$

and the angle  $\alpha$  between the normal to the reflecting plane and the axis of rotation is given by

$$(4) \quad \tan \alpha = \zeta / \xi.$$

From (1) ... (4) we have the relations giving the direction of the reflecting ray in terms of the angles  $\theta, \alpha$  as

$$(5) \quad \cos \chi \cos \phi = \cos 2\theta,$$

$$(6) \quad \sin \chi = 2 \sin \theta \sin \alpha.$$

These equations can, of course, be arrived at directly by spherical trigonometry.

In the more general case of the incident ray not being perpendicular to the axis but inclined to the equatorial plane at an angle  $\beta$ , the formulæ become more complicated, but can be derived in a similar manner from fig. 6B.

Here

$$(1') \quad \xi = \{\cos^2 \beta + \cos^2 \chi - 2 \cos \beta \cos \chi \cos \phi\}^{\frac{1}{2}},$$

$$(2') \quad \zeta = \sin \beta + \sin \chi.$$

From both (2) and (2') we see that  $\zeta$  depends only on  $\chi$ , so that all points of the reciprocal lattice of the same height above the equatorial plane, or what is equivalent, all planes of the crystal intersecting the axis at the same point give rise to reflections lying on a cone about the axis. The intersection of such cones with the photograph are the layer lines (*schichlinien*) on which the reflections of all such planes lie.

If  $\beta$  is small, (1') to the first order of small quantities takes the form (1) and (2') is unchanged. From this there follows the possibility of using as the X-ray aperture a vertical slit instead of a circular hole as not affecting the accuracy of measurement of  $\xi$ , a horizontal slit obviously fulfilling the same functions for  $\zeta$ .

We have found  $\xi$ ,  $\zeta$  in terms of the angular co-ordinates of the reflected ray; we may write these in their turn as functions of the co-ordinates of position of the corresponding spot on the photograph. The latter usually takes one of two forms—a plane plate parallel to the axis and perpendicular to the incident ray, and a cylindrical film whose axis is the axis of rotation.

Taking first the case of a plane plate at a distance  $D$  from the axis with the trace of the incident ray as origin, and the  $x$  axis in the equatorial plane (see fig. 7), we have

$$(7) \quad x/D = \tan \phi,$$

$$(8) \quad y/D = \tan \chi \sec \phi,$$

or alternatively using polar co-ordinates  $r\psi$  ( $\psi$  being measured from the  $y$  axis)

$$(9) \quad r/D = \tan 2\theta,$$

$$(10) \quad \cos \psi \cos \theta = \cos \alpha.$$

Combining with (1) (2) we have

$$(11) \quad \xi = \left\{ 2 - \frac{2}{\left(1 + \frac{r^2}{D^2}\right)^{\frac{1}{2}}} + \frac{\frac{y^2}{D^2}}{1 + \frac{r^2}{D^2}} \right\}^{\frac{1}{2}},$$

$$(12) \quad \zeta = \frac{\frac{y}{D}}{\left\{1 + \frac{r^2}{D^2}\right\}}.$$

These formulæ are sufficient to determine  $\xi$ ,  $\zeta$  from the position of the spot on the plate, but they are extremely laborious to use even for a few spots, while for the two hundred or so which may appear on a good plate it becomes almost impossible. Some means of shortening the work is therefore necessary. The most convenient formulæ for calculation are (9),

$$(12') \quad \zeta = \frac{y}{D} \cos 2\theta$$

and

$$(3') \quad \xi = \{\rho^2 - \zeta^2\}^{\frac{1}{2}} = \{4 \sin^2 \theta - \zeta^2\}^{\frac{1}{2}}.$$

From measurements of  $r$  and  $y$  we can calculate in turn  $\theta$ ,  $\zeta$ ,  $\xi$ . These calculations can be much shortened by means of a table computed by the author. The table (see end) is divided into seven columns.

Column 1 contains the values of  $\tan 2\theta = r/D$  at intervals of 0·01.

Column 2 contains the corresponding values of  $\rho = 2 \sin \theta = \lambda/d$ .

Column 3 gives for more accurate work the values of  $\cos \theta/\cos 2\theta$ . If  $r/D$

is divided by the corresponding value of  $\cos \theta/\cos 2\theta$ , we have the value of  $\rho$  (the reason this is more accurate than using the second column is that interpolation is possible owing to the slow change in the numbers).

Column 4 gives the correcting factor  $\sec 2\theta$  by which  $y/D$  must be divided to give  $\zeta$ .

Column 5 gives the value of  $\sec \theta$ .

Column 6 gives the logarithms of  $\cos \theta/\cos 2\theta$ .

Column 7 gives the logarithm of  $\sec 2\theta$ .

The last two columns are correct to four places and are given for accurate work. All the calculations may be carried out very conveniently and rapidly by the use of a slide rule. Divisions are used rather than multiplications so as to avoid the use of numbers beginning with a series of nines, which are inconvenient both for slide rule and logarithm work.

The use of the tables may be summed up in the following rules :—

Rule 1. To find  $\rho$  divide  $r/D$  by the corresponding number in Column 3.

For rough work use Column 2.

Rule 2. To find  $\zeta$  divide  $y/D$  by the number corresponding to  $r/D$  in Column 4.

Rule 3. To find  $\cos \alpha$  divide  $y/r$  by the number corresponding to  $r/D$  in Column 5.

Rule 4. To find the spacing multiply  $\lambda$  by the number corresponding to  $r/D$  in Column 3 and divide by  $r/D$ . For rough work divide  $\lambda$  by the number in Column 2 corresponding to  $r/D$ .

Rule 5. To find the cell height, multiply  $\lambda$  by the number corresponding to  $r/D$  of any spot in the first hyperbola in Column 4 and divide by  $y/D$ . If the spot is on the  $n$ th hyperbola, multiply the result by  $n$ .

Having found  $\rho$ ,  $\zeta$  we may by means of (3') calculate  $\xi$ , but a much more rapid and quite as accurate a method is to find  $\xi$  graphically from the *Rotation Diagram*. This is the name given to a diagram for which the values of  $\xi$  and  $\zeta$  are plotted as Cartesian co-ordinates. Theoretically we derive such a diagram by rotating the reciprocal lattice and marking the traces of every point as it passes through any plane containing the axis (see fig. 8). Thus the form it will take in various cases can be predicted in a very simple geometrical way. On the other hand, it can be seen from (9) (12') (3') that the values of  $\xi$ ,  $\zeta$  are

closely related to the co-ordinates  $xy$  of the spots on the plate, and are, in fact, for small angles proportional to them, so that the rotation diagram appears

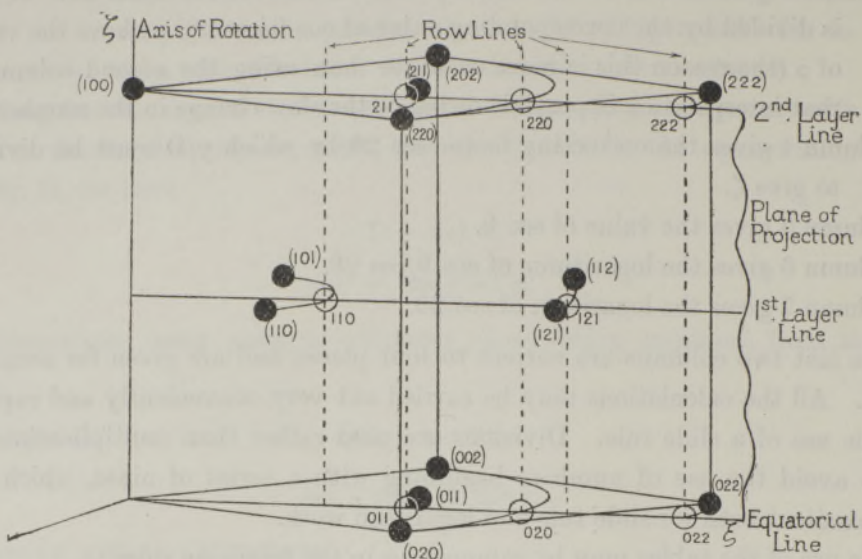


FIG. 8.—Formation of Rotation Diagram from a face-central cubic reciprocal lattice, corresponding to a body-centred crystal.

● (222) Point of reciprocal lattice. ○ 222 Point of rotation diagram.

as a modified form of the photograph itself, the fit being closest in the centre. This is what gives the rotation diagram and the co-ordinates  $\xi$ ,  $\zeta$  their great practical importance. The greatest advantage of the rotation diagram is, as will be seen later, we may by a suitable choice of axis reduce it in most cases to a rectangular framework of points, whereas on the photograph the corresponding spots lie on complicated curves.

The construction of the rotation diagram may in this case be carried out as follows (see fig. 9):—The values of  $\rho$  and  $\zeta$  for all spots on the photograph having been worked out, a piece of squared paper is taken and on it, on a suitable scale, lines are drawn parallel to the  $\xi$  axis at distances corresponding to the values of  $\zeta$  for each point. In most cases, the rotation being about a crystallographic axis, the points divide into a few sets each of which have the same value of  $\zeta$ . Here the mean value of the observed  $\zeta$  is taken and only one line drawn for each set. With the origin as centre and the radius  $\rho$ , draw arcs of circles. Where each arc cuts the corresponding  $\zeta$  line is the point on the rotation diagram corresponding to the spot on the photograph. The distance of each point from the  $\zeta$  axis gives the value of  $\xi$ . Lines may be drawn

through points parallel to the  $\zeta$  axis to indicate planes of equal  $\xi$ , i.e., planes on zones perpendicular to the rotation axis.

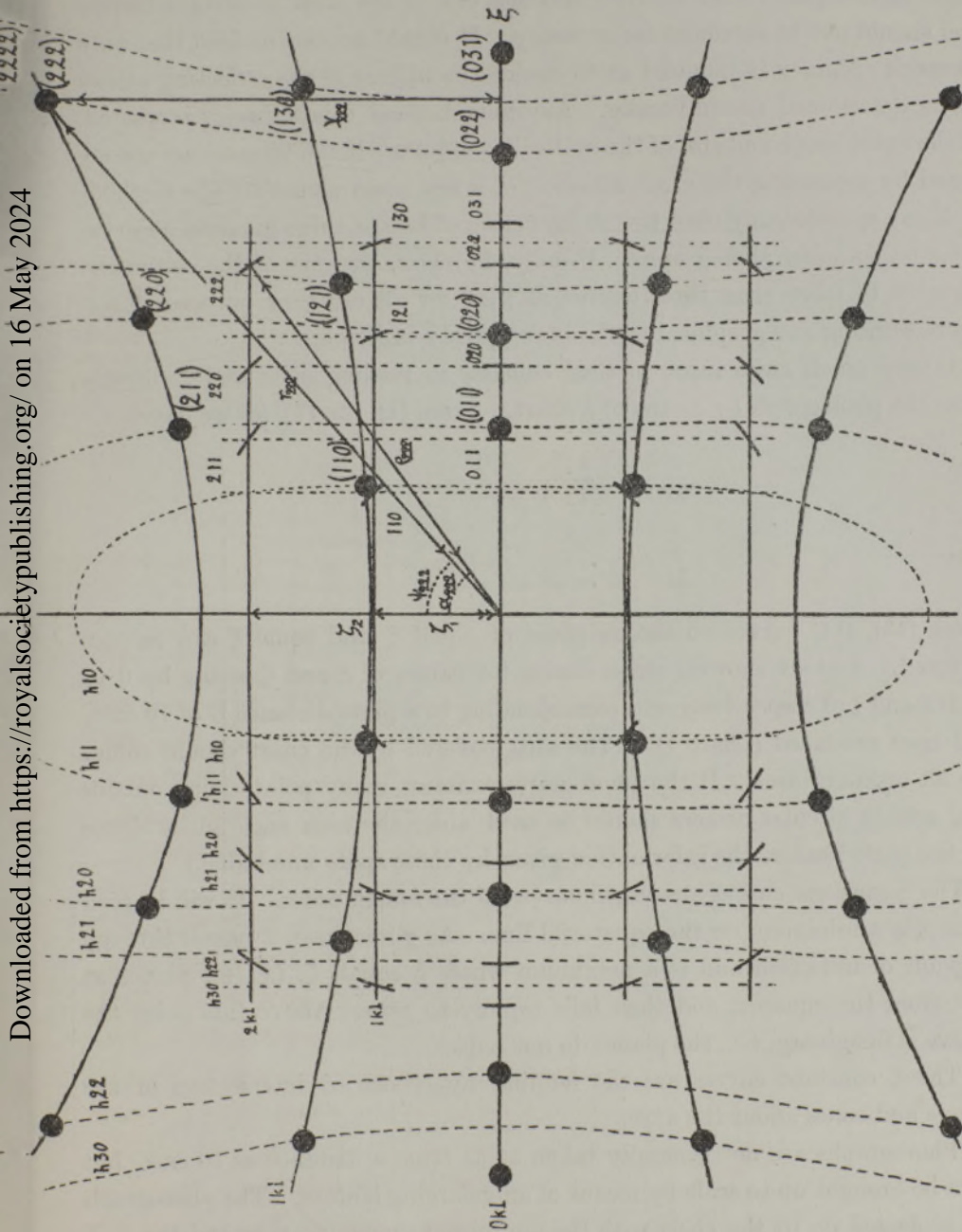


FIG. 9.—Rotation Diagram of Body-Centred Cubic Crystal rotated about its (a) axis: shown with Projection of Photograph on the same scale. (See fig. 8.)

● (222) Spot of Photograph Protection.  Point on Rotation Diagram.

This way of arriving at the values of  $\xi$  and  $\zeta$ , though much more rapid than direct calculation, still takes a considerable amount of time, for although each

set of operations is fairly short, the repeating of them from anything up to a hundred and fifty times for a good photograph may take hours of work. Time in this part of the analysis becomes one of the most important factors and should not be sacrificed for accuracy. It should be remembered that only so much accuracy is required as to enable the indices of the reflecting planes to be determined unequivocally. Anything beyond this accuracy is wasted. If the exact shape and size of the unit cell is required, it can be more accurately found by measuring the exact spacings of a few main planes by the methods of X-ray spectroscopy than by the averaging of two or three hundred observations on rotation photographs. Usually, however, the size of the cell is not required to more than three figures, so that for all ordinary purposes three-figure working and graphical methods are quite admissible.

A very much more rapid method consists in reading off  $\xi$  and  $\zeta$  directly from the photograph by means of a chart. From (1), (2), (7), (8) we have

$$(13) \quad \frac{x}{D} = \left\{ \frac{4(1 - \zeta^2)}{(2 - \rho^2)^2} - 1 \right\}^{\frac{1}{2}},$$

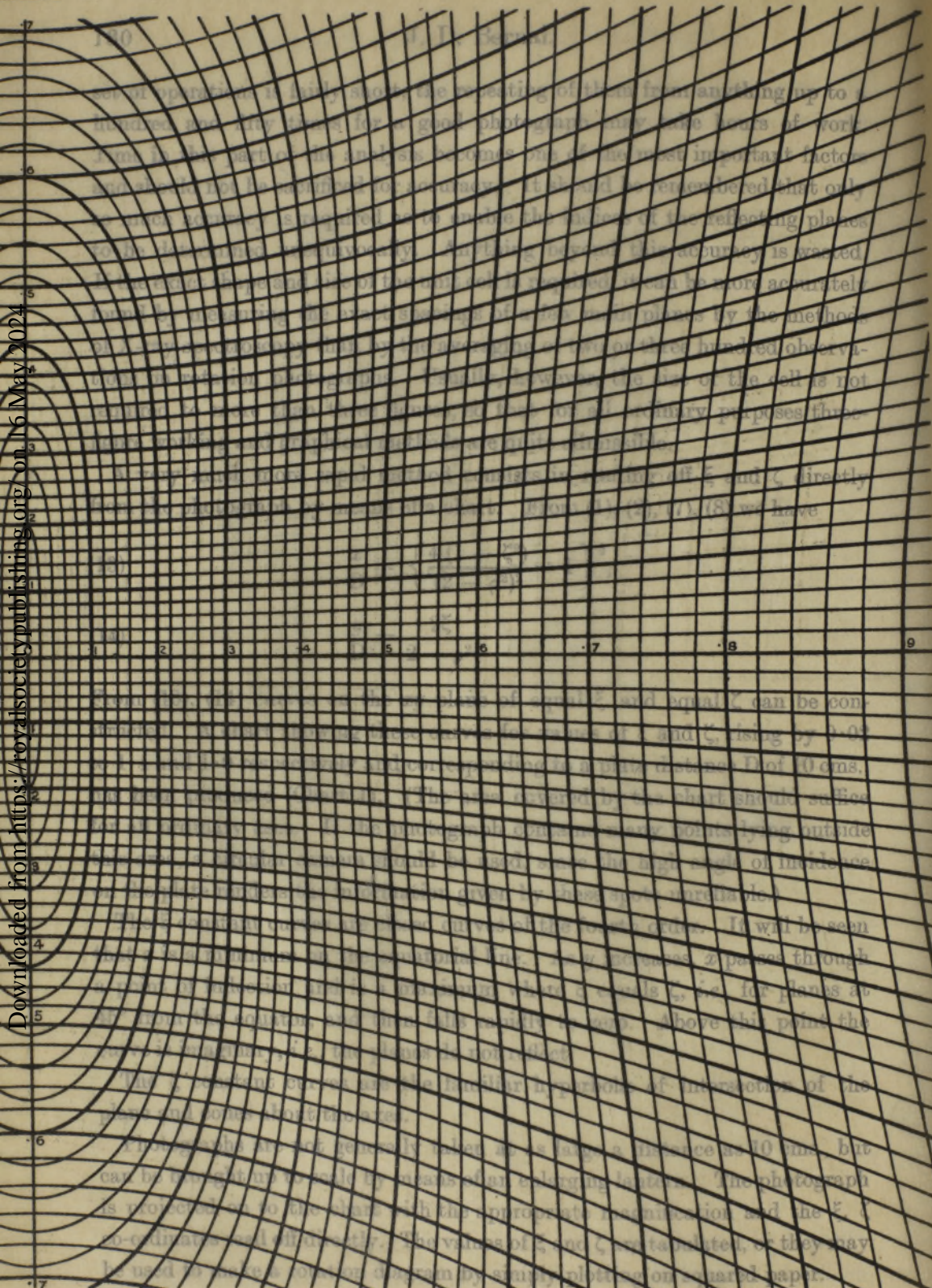
$$(14) \quad \frac{y}{D} = \frac{2\zeta}{2 - \rho^2}.$$

From (13), (14) curves on the  $xy$  plane of equal  $\xi$  and equal  $\zeta$  can be constructed. A chart showing these curves for values of  $\xi$  and  $\zeta$ , rising by 0.02 to 1.4 and 1.0 respectively and corresponding to a plate distance  $D$  of 10 cms., has been produced (Chart 1). (The area covered by the chart should suffice for all ordinary uses. If the photograph contains many points lying outside this area, a circular camera should be used, since the high angle of incidence on the plate renders the information given by these spots unreliable.)

The  $\xi$  constant curves are closed curves of the fourth order. It will be seen that  $x$  is a minimum on the equatorial line. As  $y$  increases,  $x$  passes through a point of inflection and is a maximum where  $\xi$  equals  $\zeta$ , i.e., for planes at  $45^\circ$  from the equator, and then falls rapidly to zero. Above this point the curve is imaginary, i.e., the planes do not reflect.

The  $\zeta$  constant curves are the familiar hyperbolæ of intersection of the plane and cones about the axes.

Photographs are not generally taken at as large a distance as 10 cms., but can be brought up to scale by means of an enlarging lantern. The photograph is projected on to the chart with the appropriate magnification and the  $\xi$ ,  $\zeta$  co-ordinates read off directly. The values of  $\xi$  and  $\zeta$  are tabulated, or they may be used to make a rotation diagram by simply plotting on squared paper.



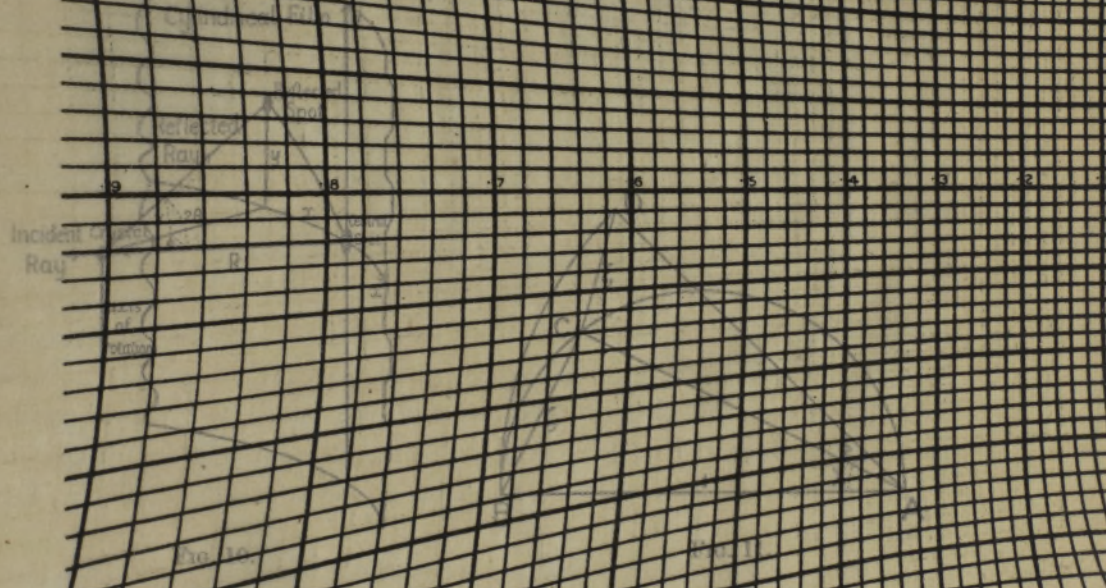
The values of  $\alpha$  are sometimes required for purposes of setting. They may be found from the table by rule 3, or from the chart where  $\tan \alpha = \frac{r}{l}$ , and of course one may read directly off the rotation diagram being merely like angle between the radius vector and the  $x$ -axis.

In the case of a cylinder of radius  $R$  and  $l$  length given directly by

$$(15) \quad \alpha = \arctan \frac{R}{l}$$

$$(16) \quad \alpha = \arctan \frac{r}{l}$$

where  $r$  is the distance before the crystal of the point at which the cylinder passes through it. We wish to find the angle  $\alpha$  between



but the formula is clumsy and it is easier to calculate  $r/l$  and find  $\alpha$  from  $r/l$ . The calculations are laborious, and for practical purposes it is sufficient to use a graphical construction with a modification of the rule to Spherical. On a line of unit length  $AB$  describe a semicircle above  $A$  making an angle  $\alpha$  with  $AB$  and cutting the semicircle at  $C$ . Draw  $AC$  of unit length making an angle  $\alpha$  with  $AC$ . Then

$$BC = \sin \alpha = r/l$$

and

$$CD = \sqrt{1 + \cos^2 \alpha - 2 \cos \alpha \cos \beta} = \frac{r}{l} \text{ (see fig. 11)}$$

The values of  $\alpha$  are sometimes required for purposes of setting. They may be found from the tables by rule 3, or from the chart where  $\tan \alpha = \zeta/\xi$ , and of course  $\alpha$  may be read directly off the rotation diagram, being merely the angle between the radius vector and the  $\zeta$  axis.

In the case of a cylindrical camera of radius  $R$ ,  $\chi$  and  $\phi$  are given directly by

$$(15) \quad x/R = \phi,$$

$$(16) \quad y/R = \tan \chi,$$

where  $x$  and  $y$  as before are Cartesian co-ordinates taken on the developed cylindrical film (see fig. 10). We might combine these as before with (1), (2),

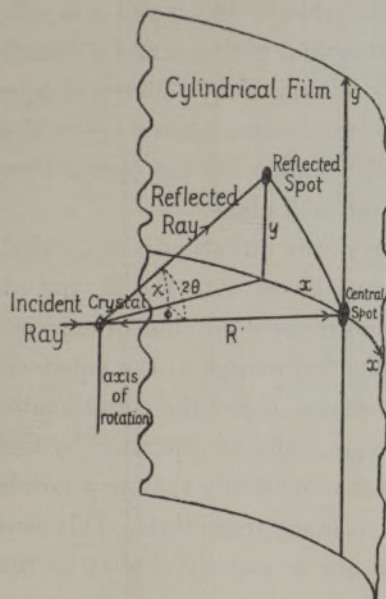


FIG. 10.

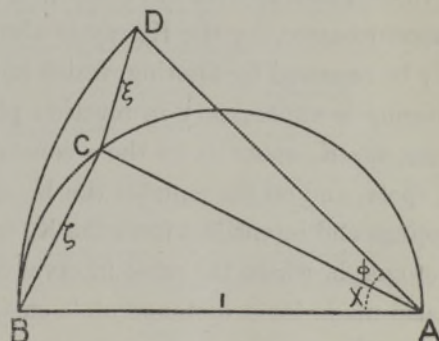


FIG. 11.

but the formulæ are clumsy and it is easier to calculate  $\chi$ ,  $\phi$  and from them  $\xi$ ,  $\zeta$ . The calculations are laborious, and for practical purposes it is sufficient to use a graphical construction which is a modification of that due to Schiebold. On a line of unit length AB describe a semicircle; draw a line AC making an angle  $\chi$  with AB and cutting the semicircle at C. Draw AD of unit length making an angle  $\phi$  with AC; then

$$BC = \sin \chi = \zeta,$$

and

$$CD = \{1 + \cos^2 \chi - 2 \cos \chi \cos \phi\}^{\frac{1}{2}} = \xi \text{ (see fig. 11).}$$

This method, though quicker than calculation, is still rather slow and, as in the case of the plane plate, a chart has been constructed to give the values of  $\xi$  and  $\zeta$  directly. This chart (Chart 2) is in every way similar to the one for the plane plate except that here the  $\zeta$  constant curves are straight lines. The chart is constructed for a cylindrical camera of radius 5 cms. The  $\zeta$  values rise by 0.05 to 0.9; the  $\xi$  values by 0.05 to 2. A more open scale is necessary on account of the greater field covered. The use of this chart is exactly the same as that of Chart 1.

The values of  $\theta$  and  $\alpha$  cannot be calculated rapidly from the co-ordinates of a cylindrical film. It is best to calculate in two stages by means of (15), (16), (5), (6). The values can, of course, be found from Chart 2 as before, but often, particularly for setting purposes, it is desirable to find  $\theta$  and  $\alpha$  rapidly. For this another chart (Chart 3) has been constructed, giving  $\theta$  and  $\alpha$  directly for every  $5^\circ$ . The curves  $\theta$  constant are the ordinary Debye curves of equal spacing. The  $\alpha$  constant curves are similar to lemniscates when  $\alpha$  is less than  $45^\circ$  and are sinuous when  $\alpha$  is greater than  $45^\circ$ . They are the curves along which the spectra of the incident radiation lie for each plane.

N.B.—These spectra are important in so far as the radiation is not strictly monochromatic, for the  $K_\beta$  ray is always present along with the  $K_\alpha$  and can only be removed by filtering, which increases enormously the time of exposure. Filtering is unnecessary in rotation photographs for, except in the equatorial plane, the  $K_\beta$  spots lie on the  $\alpha$  constant lemniscates below the corresponding  $K_\alpha$  spots, and on the equator the  $K_\beta$  spots can generally be separated by their spacings and intensities from the  $K_\alpha$  spots much more easily than in a powder photograph, where the same interval contains so many more lines. This chart is also made for a distance of 5 cms. and its use is exactly similar to that of the others.

We have so far limited ourselves to the case of a single reflecting plane. When we come to deal with the crystal as a whole, we must consider first of all its setting, that is, the relation of the axis of rotation to the crystallographic axes. As might be expected, the choice of a crystallographic axis itself gives by far the simplest result, but it is necessary under certain circumstances to set the crystal in other crystallographic or non-crystallographic directions. For this purpose the apparatus should be provided with goniometrical setting arcs so that the setting of the crystal can be achieved with at least goniometrical accuracy. It may be useful at this point to enumerate some other necessary characters of any apparatus with which reliable results can be obtained :

- (1) The breadth and divergence of the incident beam of X-rays must be controllable.
- (2) The axis of this beam must be perpendicular to the axis of rotation and must intersect it at the point where the crystal is placed.
- (3) The crystal must be capable of being centred on the axis of rotation and set at any desired angle to the axis of rotation and to the incident beam.
- (4) The plate should be in its usual position normal to the incident beam or the cylindrical camera should have the axis of rotation as its axis.

The accuracy attainable should be within a few minutes of arc in each case.

If the crystal has developed faces the setting may be effected by ordinary goniometrical methods. In a large number of cases, however, either no faces or very imperfect faces are developed. In this case the setting itself must be effected by X-rays. It is impossible to give details here, but the principle of the method is to set the crystal in any position, select a reflection, preferably one with the largest spacing, find the  $\alpha$  angle of the corresponding plane, move the crystal through a known angle on the setting arcs, take another photograph, find the new  $\alpha$  angle, and by means of the two  $\alpha$  angles work out by spherical trigonometry the angles through which the crystal must be turned to bring one of its axes into coincidence with the axis of rotation. Laue methods can also be used for this purpose with advantage.<sup>†</sup>

We have chosen  $\xi$  and  $\zeta$  to be the cylindrical co-ordinates of points of the reciprocal lattice referred to the axis of rotation. If now we choose as axis of rotation any primitive translation  $a$ , say, of the original lattice, this is equivalent to choosing an axis perpendicular to the  $b^*c^*$  plane in the reciprocal lattice. The points in the reciprocal lattice will then be arranged in layers parallel to this equatorial plane. Each of these layers will be characterised by the same value of the index  $h$  and the same value of  $\zeta$ , so that we have the relation

$$a = h\lambda/\zeta.$$

If, therefore, the axis is taken along a primitive translation of the crystal, *i.e.*, along a zone axis, the spots on the photograph will all lie on a series of lines of equal  $\zeta$ , which may be called layer lines accordingly.

By measuring the  $\zeta$ 's for these lines we can determine the length of the primitive translation unequivocally. If we take the axes along each of the crystal axes  $a$ ,  $b$ ,  $c$ , in turn, we can thus measure the size of the unit cell.

The procedure is as follows : from the photograph taken about a crystallo-

<sup>†</sup> See Bernal, 'Roy. Soc. Proc.,' A, vol. 106, p. 749 (1924).

graphic axis,  $a$ , say, as rotation axis, the  $\zeta$  value of each line of spots  $\zeta_1, \zeta_2, \dots$ , is determined by the average of a few spots in each line. Then  $a$  is given by the average of  $\lambda/\zeta_1, 2\lambda/\zeta_2, \dots$ . Very great care should be taken to see that no spots lie between the lines chosen (except, of course, the  $K_s$  spots, whose intensity and position make their detection easy; see p. 132). In a great number of crystals there is a tendency for the lines of odd orders, 1st, 3rd, etc., to have very weak spots and few of them. The tendency is less marked in the 3rd than in the 1st, in the 5th than in the 3rd, and so on, so that it is in these higher order lines that the spots should be looked for.\* Failure to notice these spots will lead to a false unit cell whose length in the particular direction chosen is half that of the true unit cell.

In the case of crystals of orthogonal systems, *i.e.*, cubic, tetragonal, hexagonal, trigonal and orthorhombic crystals, photographs of rotations about the three principal axes give the three axial lengths  $a, b, c$  of the orthogonal cell. On account of the symmetry one photograph is sufficient in the cubic system and two in the tetragonal, hexagonal and trigonal systems. The orthogonal cell is the same or different from the true unit cell, according as the lattice belongs to the  $\Gamma$  or to one of the  $\Gamma'$  types. To distinguish between the various lattice types, the criterion is the absence of some of the general planes  $h, k, l$ . If for any reason there should be any doubt as to the type of lattice, a rotation photograph about the [110] or [111] directions will soon settle it. In the [110] photograph the odd-layer lines, as calculated from the orthogonal cell, vanish for a face-centred lattice. In the [111] photograph they vanish for a body-centred lattice.

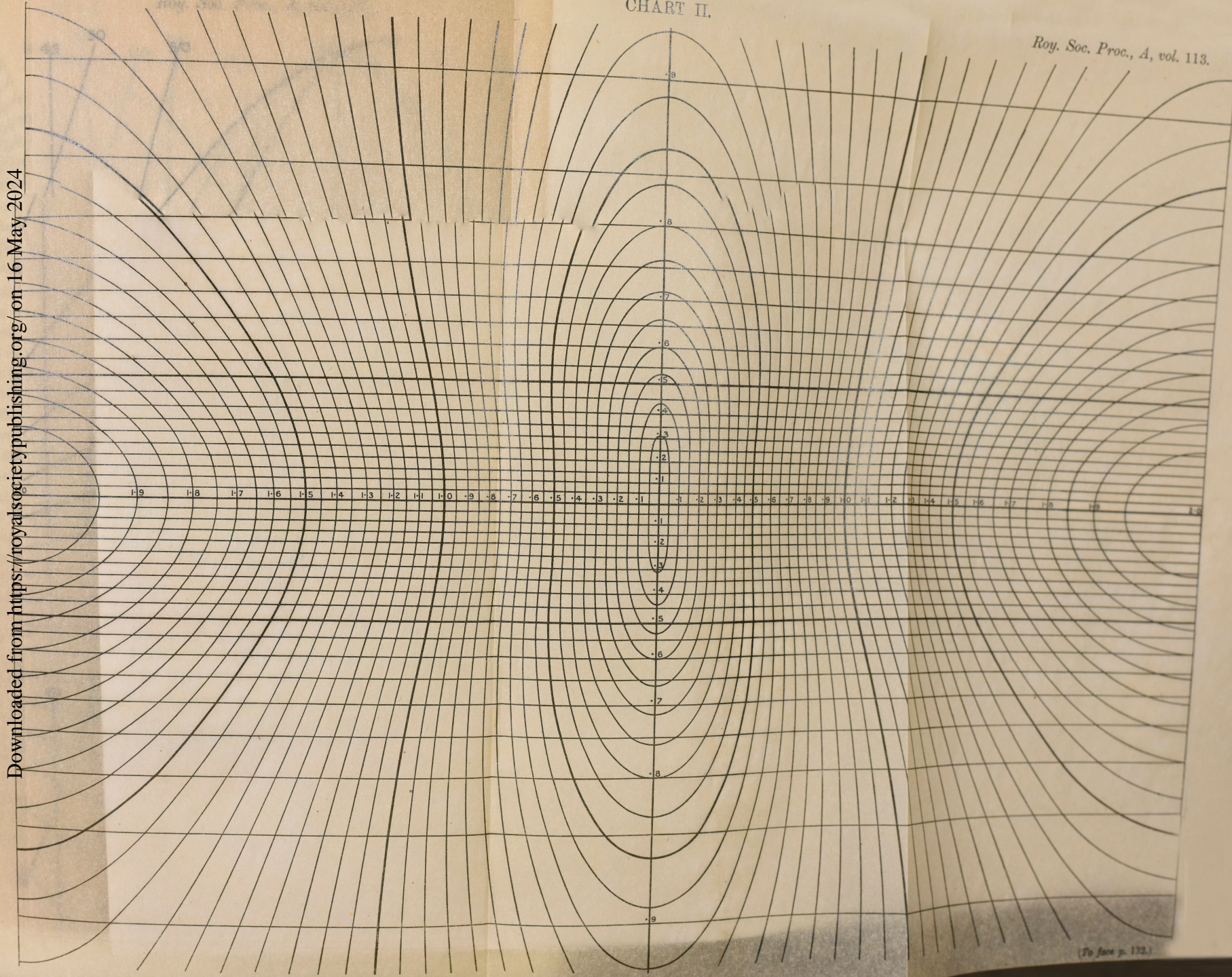
In the case of monoclinic and triclinic crystals the correct unit cell is harder to find because the crystallographic axes  $a, b, c$  do not bear a known relation to the three primitive translations which define the unit cell. The  $b$  axis can, of course, be measured as before, but the true  $a$  and  $c$  axes can be chosen arbitrarily, the only stipulation being that they should be primitive to each other, *i.e.*, that the parallelogram  $ac$  should contain no other points of the lattice. This might be decided by taking photographs about other axes in the  $ac$  plane, but the process is laborious. It is easier to proceed by taking as  $a$  and  $c$  axes any two prominent crystallographic directions and working out the indices  $h, k, l$  on the basis of this lattice. If several sets of indices are missing, and if all those that appear can be made to fit in with a formula of the type

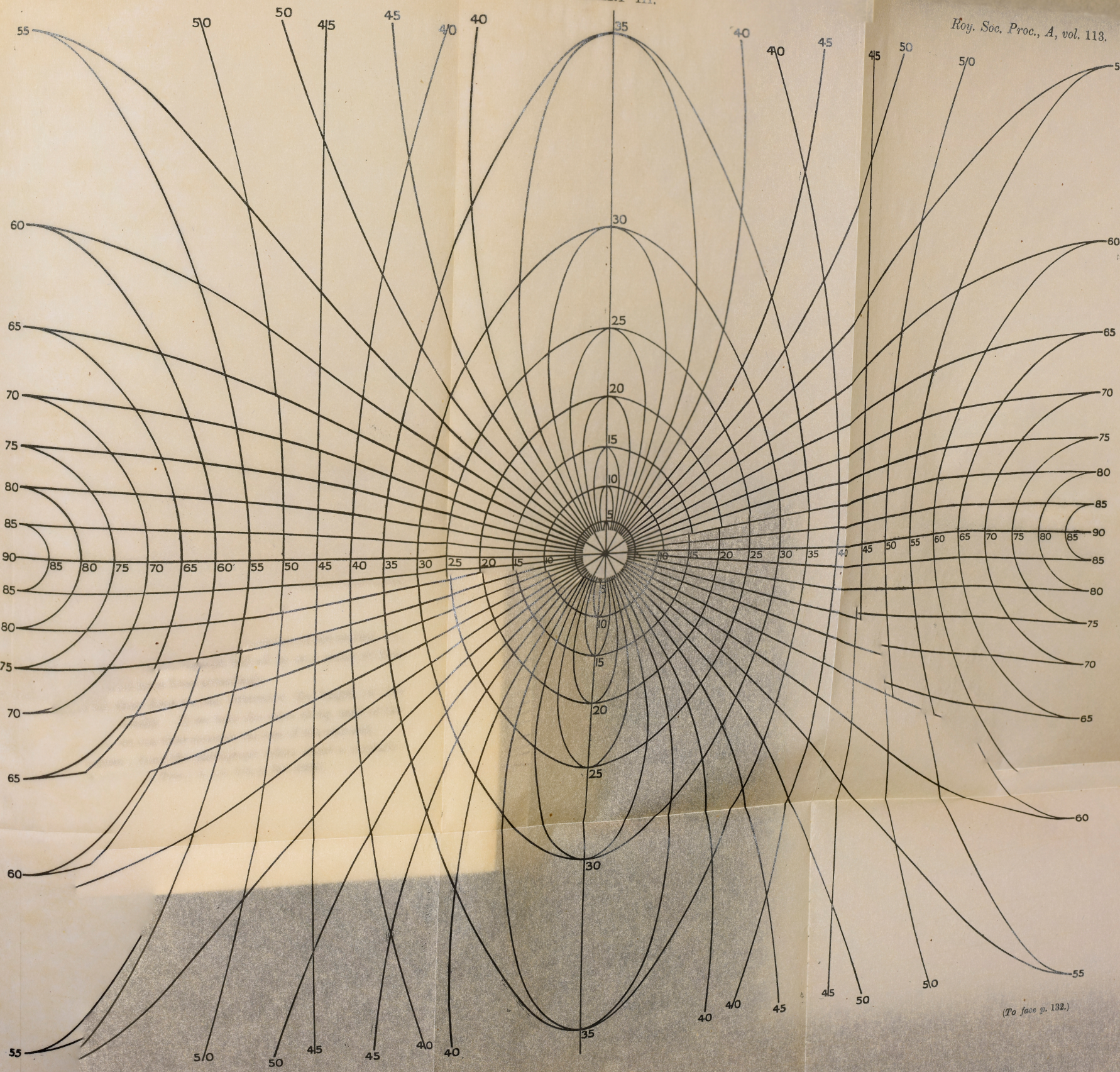
$$k'h + l'l = nj,$$

\* See Astbury, 'Roy. Soc. Proc.,' A, vol. 122, p. 216 (1926).—Added in proof.

CHART II.

Roy. Soc. Proc., A, vol. 113.





where  $h'$ ,  $l'$  are constant integers and  $n$  is any integer, then the wrong  $a$  and  $c$  axes have been chosen, the correct ones being given in vector notation by

$$\mathbf{a}' = \mathbf{a},$$

$$\mathbf{c}' = \frac{h'\mathbf{a} - l'\mathbf{c}}{j}.$$

The same applies to the triclinic system, but in this case three instead of two axes can be chosen in an arbitrary manner. As before, the best way is to choose three crystallographic directions and work out the indices, taking these as  $abc$ . If only certain sets of planes appear, the axes can be changed so that all types of planes are represented. The cases occurring in practice are usually so simple that general formulæ are not given here.

After the determination of cell size the next problem is that of the indices of the spots. We will first consider the case of orthogonal crystals, *i.e.*, cubic, tetragonal, hexagonal, trigonal and orthorhombic crystals. For trigonal and hexagonal crystals it is most convenient for rotation photographs to use orthohexagonal co-ordinates. The crystals are referred to three orthogonal axes  $a$ ,  $b = \sqrt{3}a$  and  $c$ . This method, of course, loses sight of the trigonal symmetry, but it enables these two systems to be brought into line with the other orthogonal systems. The symmetry does not appear in rotation photographs directly, and the calculations, using hexagonal co-ordinates, are complicated.

If an orthogonal crystal be rotated about a principal axis, the  $a$  axis, say, the  $\xi$ ,  $\zeta$  co-ordinates of the spot corresponding to the plane  $(hkl)$  are

$$\xi = \lambda \left\{ \frac{k^2}{b^2} + \frac{l^2}{c^2} \right\}^{\frac{1}{2}}, \quad \zeta = \frac{\lambda h}{a},$$

or if we take the primitive translations of the reciprocal lattice

$$a^* = \lambda/a, \quad b^* = \lambda/b, \quad c^* = \lambda/c,$$

we have

$$(17) \quad \xi = \{k^2 b^{*2} + l^2 c^{*2}\}^{\frac{1}{2}},$$

$$(18) \quad \zeta = \hbar a^*.$$

One co-ordinate of a spot always appears from its position on one or other of the layer lines; the others have to be found by a process analogous in two dimensions to what the identification of powder photographs is in three.  $b^*$  and  $c^*$  being known ( $b^* = \zeta_b$ ;  $c^* = \zeta_c$  of the layer lines on the rotation photograph about the  $b$  and  $c$  axis respectively), it is easy to make a list of theoretical  $\xi$ 's for all integral values of  $k$  and  $l$  which give values of  $\xi$  within

the range of the photographs. For each layer line, *i.e.*, for  $h = 0, 1, 2, \dots$  planes may be looked for having  $\xi$  equal to one of the theoretical values. The  $h, k$  number corresponding to this value give the other two indices of the spot.

Graphically, this is equivalent to drawing lines on the rotation diagram parallel to the  $\zeta$  axis at distances equal to the radii vectors of the points in the reciprocal net of the  $b, c$  plane. It can best be carried out in two stages (see fig. 12). The first is the drawing of this reciprocal net (this may be reduced to merely two lines at right angles divided in intervals of  $b^*$  and  $c^*$  if the oscillation method is not going to be employed). The second stage consists of marking off along the  $\xi$  axis of the rotation diagram the  $\xi_{h,l}$  distances from the net diagram. From these points lines are drawn parallel to the  $\zeta$  axis. Such lines for which  $h, l$  and  $\xi$  are constant are called row lines; they correspond to a row of points in the reciprocal lattice parallel to the axis. Layer lines are drawn through the points  $a^*, 2a^*, \dots$  parallel to the  $\xi$  axis. The intersections of the row lines and layer lines give all the theoretically possible points in the rotation diagram, and the indices of the actually observed spots may be read off directly by their coincidences with these points.

If the different values of  $\xi$  were always separated by sufficient intervals to enable the spots corresponding to them to be resolved apart, the identification of indices would be unequivocal. This is the case in the cubic system for planes whose indices are not very great, and in the tetragonal, hexagonal and trigonal systems taken about their principal or  $c$  axis. Here the  $a$  and  $b$  axial lengths being equal or their squares commensurate (17) takes the form

$$(17') \quad \xi = a^* \{h^2 + k^2\}^{\frac{1}{2}}$$

for the cubic system, or

$$(17'') \quad \xi = a^* \left\{ h^2 + \frac{k^2}{3} \right\}^{\frac{1}{2}}$$

for the trigonal and hexagonal systems, so that the difference between successive values of  $\xi$  can never be less than

$$a^* \{ \sqrt{n+1} - \sqrt{n} \} \quad \text{or} \quad a^*/\sqrt{3} \{ \sqrt{n+1} - \sqrt{n} \},$$

where  $n$  is an integer. It is only for large values of  $n$  that the minimum distance becomes small.

These restrictions do not, of course, operate among orthorhombic crystals nor in tetragonal, hexagonal or trigonal crystals rotated about their  $a$  or  $b$  axes. Here very often among planes of comparatively low indices there are

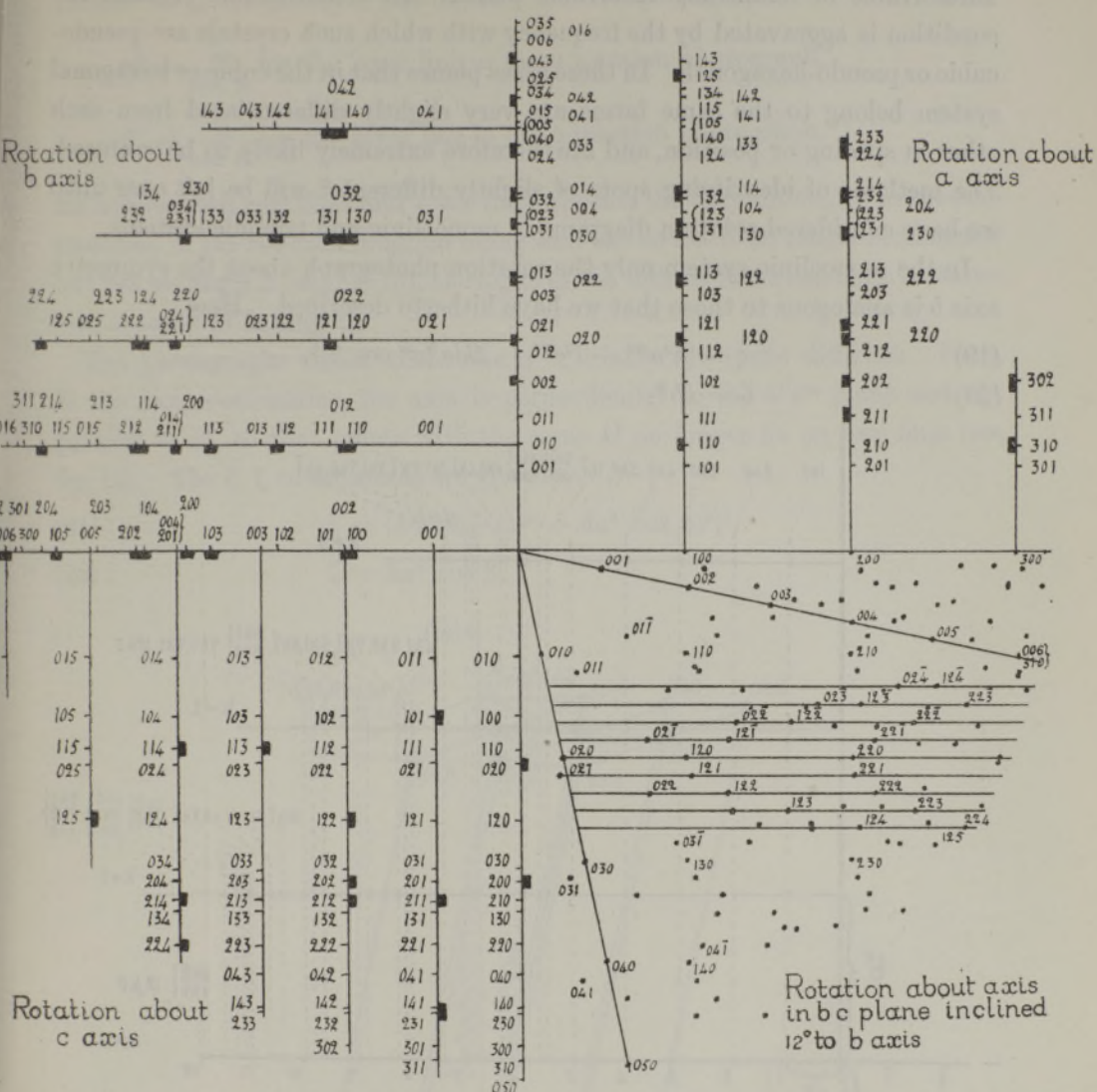


Fig. 12.—Triple Rotation Diagram about  $a$ ,  $b$  and  $c$  axis of Typical [Orthorhombic] Crystal ( $\beta$ -form of Gallium Acetylacetate).  $a^* = 0.187$ ,  $b^* = 0.120$ ,  $c^* = 0.096$ .  $\lambda_{K\alpha} = 1.54$  A.V.

Layer Line.

Observed Points.      Theoretical Points.

(Row Lines not shown.)

unresolvable or doubtfully resolvable planes. In orthorhombic crystals the condition is aggravated by the frequency with which such crystals are pseudo-cubic or pseudo-hexagonal. In these cases planes that in the cubic or hexagonal system belong to the same forms are very slightly differentiated from each other in spacing or position, and are therefore extremely likely to be confused. The methods of identifying spots of slightly different  $\xi$  will be left over until we have considered rotation diagrams in monoclinic and triclinic systems.

In the monoclinic system only the rotation photograph about the symmetry axis  $b$  is analogous to those that we have hitherto described. Here

$$(19) \quad \xi = \{h^2 a^{*2} + l^2 c^{*2} - 2hla^*c^* \cos \beta\}^{\frac{1}{2}},$$

$$(20) \quad \zeta = kb^*.$$

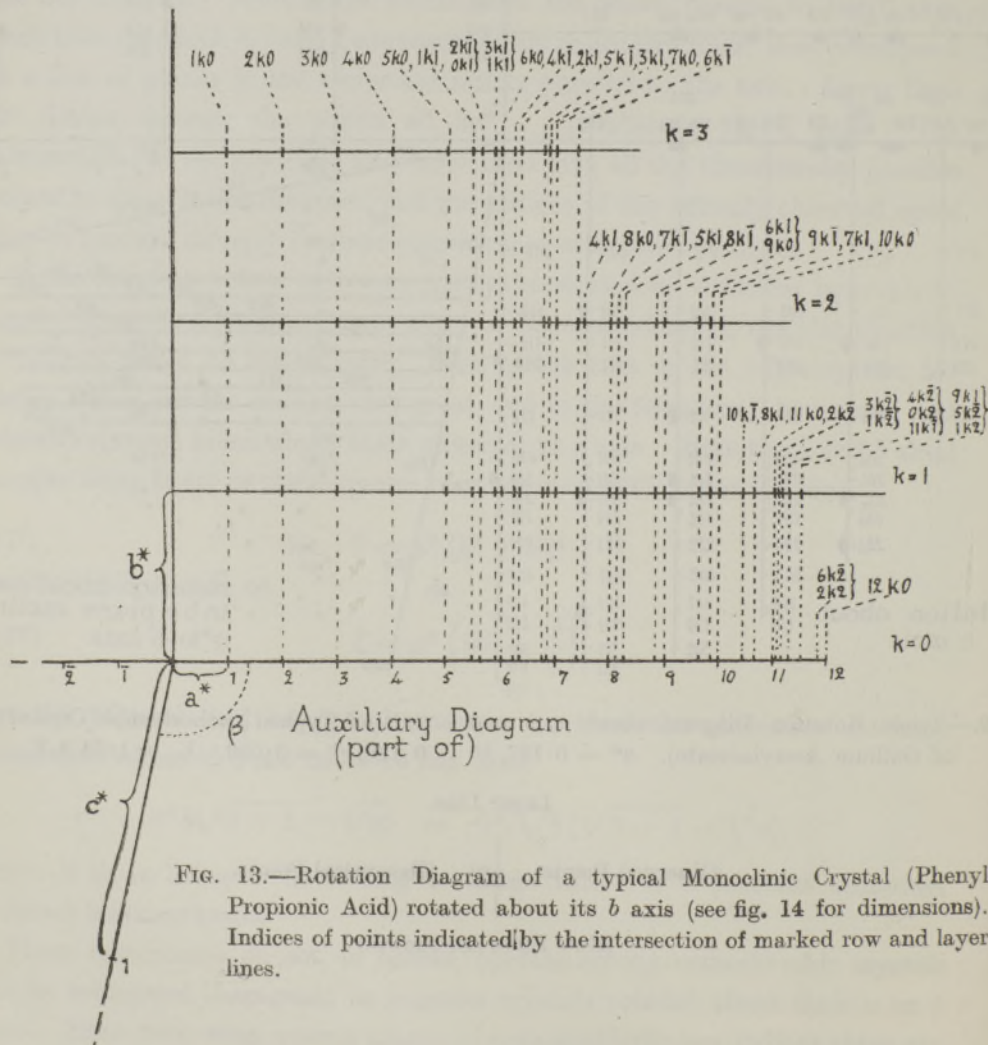


FIG. 13.—Rotation Diagram of a typical Monoclinic Crystal (Phenyl Propionic Acid) rotated about its  $b$  axis (see fig. 14 for dimensions). Indices of points indicated by the intersection of marked row and layer lines.

Here  $b^* = \zeta_b$  for the layer line in the  $b$  rotation photograph,

$$a^* = \frac{\zeta_a}{\sin \beta} \text{ for the layer line in the } a \text{ rotation photograph,}$$

$$c^* = \frac{\zeta_c}{\sin \beta} \text{ for the layer line in the } c \text{ rotation photograph.}$$

As before, both row lines and layer lines appear, the only difference in the construction of the rotation diagram being that the  $ac$  net is no longer rectangular but has an angle  $\beta$  (see fig. 13), the signs of the indices must therefore be taken into account in finding  $\xi_{hl}$ .

The photographs taken about the  $a$  or  $c$  axes are quite different. Here, in the reciprocal lattice, the axis is perpendicular to the  $b^*c^*$  plane and not parallel to  $a^*$ , so that points with the same  $kl$  no longer lie on row lines (see fig. 14). The  $\xi, \zeta$  co-ordinates are given by

$$(21) \quad \xi = \{k^2 b^{*2} + (lc^* + ha^* \cos \beta)^2\}^{\frac{1}{2}},$$

$$(22) \quad \zeta = ha^* \sin \beta.$$

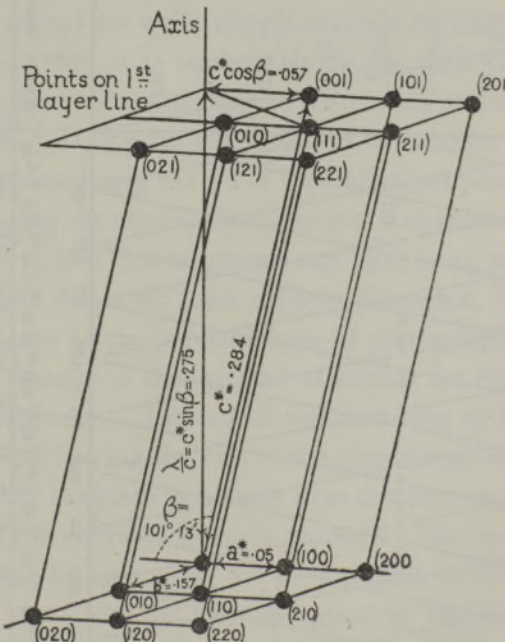


FIG. 14.—Reciprocal Lattice of typical Monoclinic Crystal (Phenyl Propionic Acid) rotated about its  $c$  axis.

From (21), (22) it can be seen that if  $k, l$  are constant the points  $(hkl)$  lie on a hyperbola whose formula is

$$\xi^2 - \zeta^2 \cot^2 \beta - 2\zeta lc^* \cot \beta - k^2 b^{*2} - l^2 c^{*2} = 0.$$

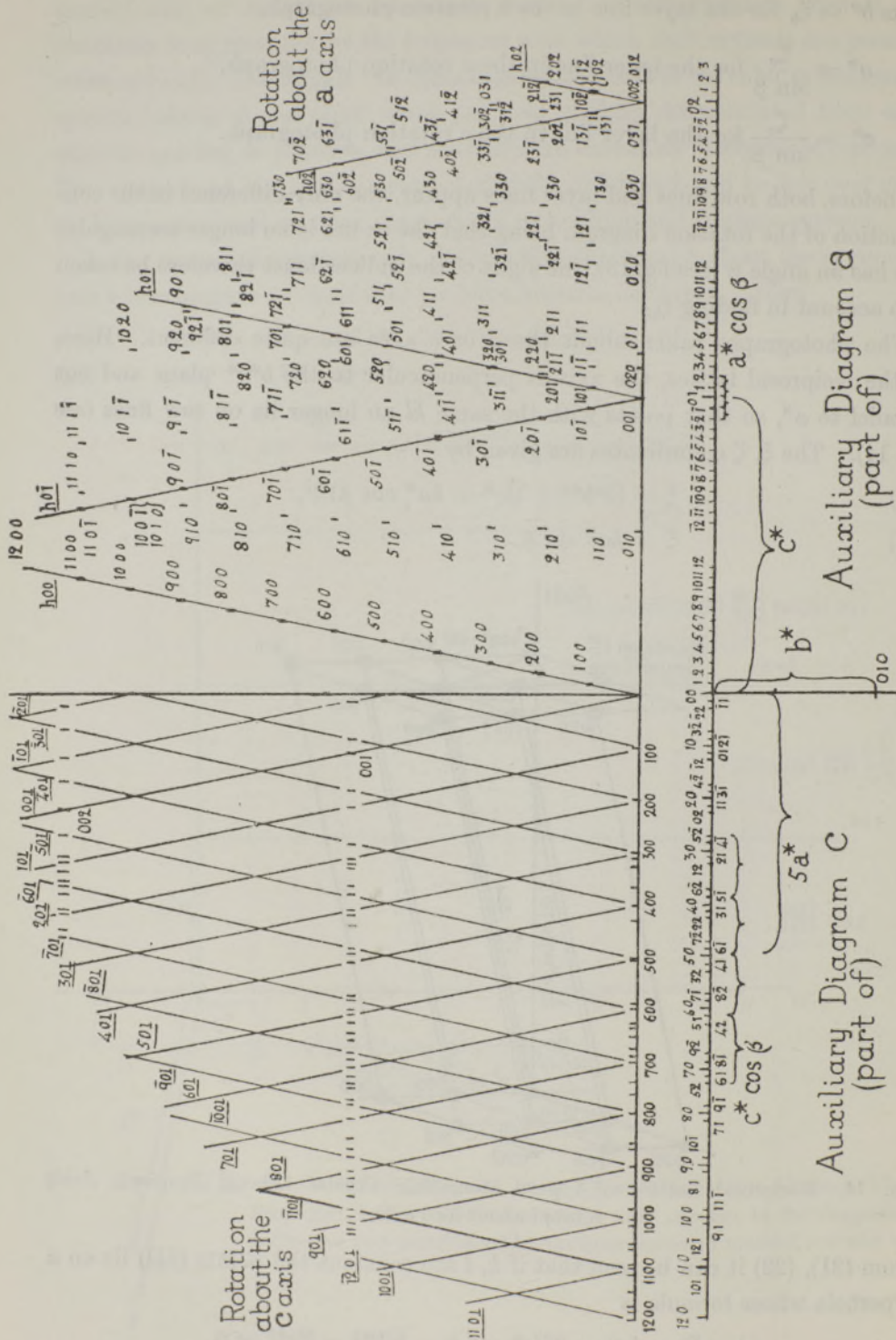


FIG. 15.—Rotation Diagrams of typical Monoclinic Crystal (Phenyl Propionic Acid) rotated about its *a* and *c* axes.

These hyperbolæ have for apices the points  $kb^*$ ,  $-lc^* \tan \beta$  and for asymptotes the lines  $\xi \pm (\zeta \cot \beta + lc^*) = 0$ , which are a particular case of the hyperbola when  $k = 0$  (see fig. 15). Thus only the set of planes  $(h0l)$  where  $l$  is constant lie on straight lines on the rotation diagram. In this case more than in the previous ones graphical methods are preferable to calculation. The  $b^*c^*$  net is drawn as before, but in addition we mark off along the  $c^*$  axis divisions equal to  $a^* \cos \beta$ . The rotation diagram has, as before, layer lines, but the row lines have disappeared. On the  $h = 0$  layer line we mark off the  $\xi_{kl}$ 's from the net as before, but on the layer line  $h = n$  we measure off the  $\xi_{kl}$ 's not from the origin of the net but from the  $n$ th new divisions on the  $c^*$  axis, the division one side of the origin corresponding to the plane  $(nkl)$ , that on the other to  $(\bar{n}kl)$  (see fig. 15).

The setting up of monoclinic crystals with their  $a$  and  $c$  axes along the axis of rotation is for the determination of indices even more liable to lead to unresolvable spots than in the case of orthorhombic crystals. Photographs should, of course, always be taken with such settings for the determination of axial lengths, but except for quite simple crystals or where either the  $c$  or  $a$  axis is long (see fig. 15a), it is inadvisable to use such photographs for the determination of indices. For this purpose the method presently to be described is much more suited. It is generally sufficient to measure only the  $\zeta$ 's of the layer lines without considering the  $\xi$ 's of the individual points at all.

If instead of rotating the crystal about the  $a$  or  $c$  axes it is rotated about the normal to the  $(100)$  or  $(001)$  (or in general any  $(h0l)$  face), we obtain a type of photograph in which the layer lines entirely disappear, but where the row lines, which are absent in the previous type of photograph, are brought into evidence. The advantage of this method of setting for the determination of indices is at once apparent. Instead of concentrating all the spots on three or four layer lines and leaving the rest of the photograph empty, we have the spots distributed over the plate in a fairly even manner, so that the likelihood of two spots being unresolvable is much reduced. This method of setting is equivalent to taking the axis along the  $a^*$  direction in the reciprocal lattice so that all rows of spots with the same  $kl$  appear on the diagram as row lines (see fig. 16). On the other hand, nets of points parallel to the  $b^*c^*$  plane no longer give layer lines, though those points with the same  $hl$  co-ordinates still do so.  $\xi$  and  $\zeta$  are given by

$$(23) \quad \xi = \{k^2 b^{*2} + l^2 c^* \sin^2 \beta\}^{\frac{1}{2}},$$

$$(24) \quad \zeta = ha^* - lc^* \cos \beta.$$

Here again the graphical method is best. The basal net is rectangular as before, but here the divisions are  $b^*$  and  $c^* \sin \beta$  (see fig. 17). From it we can

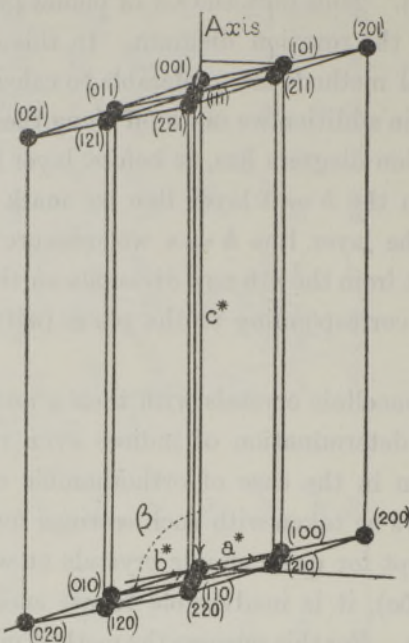


FIG. 16.—Reciprocal Lattice of typical Monoclinic Crystal rotated about the normal to the (001) plane.

mark off the positions of the row lines  $kl$ . For layer lines we draw the double series of lines making intercepts of  $ha^* - lc^* \cos \beta$ , where each of these lines meets the row line of the same  $l$  is the position of the point  $(hkl)$ . It will be seen that the position of a point now gives all three indices in a more direct manner: the  $a$  and  $c$  indices from  $\zeta$  and the  $b$  index from  $\xi$  and a knowledge of the  $c$  index, thus affording an additional check for the latter.

The case of triclinic crystals is similar though naturally more complicated. Here again photographs may be taken with the rotation axis parallel to a zone axis or perpendicular to a face. The latter method is considerably shorter and less liable to unresolved spots, but both are described here, as rotations about zone axes should always be taken to determine the cell size, and may occasionally be the only photographs available.

In the triclinic system the axes of the reciprocal lattice are given in terms of those of the crystal lattice by :

$$a^* = \frac{\lambda \sin \alpha}{Na}, \quad b^* = \frac{\lambda \sin \beta}{Nb}, \quad c^* = \frac{\lambda \sin \gamma}{Nc},$$

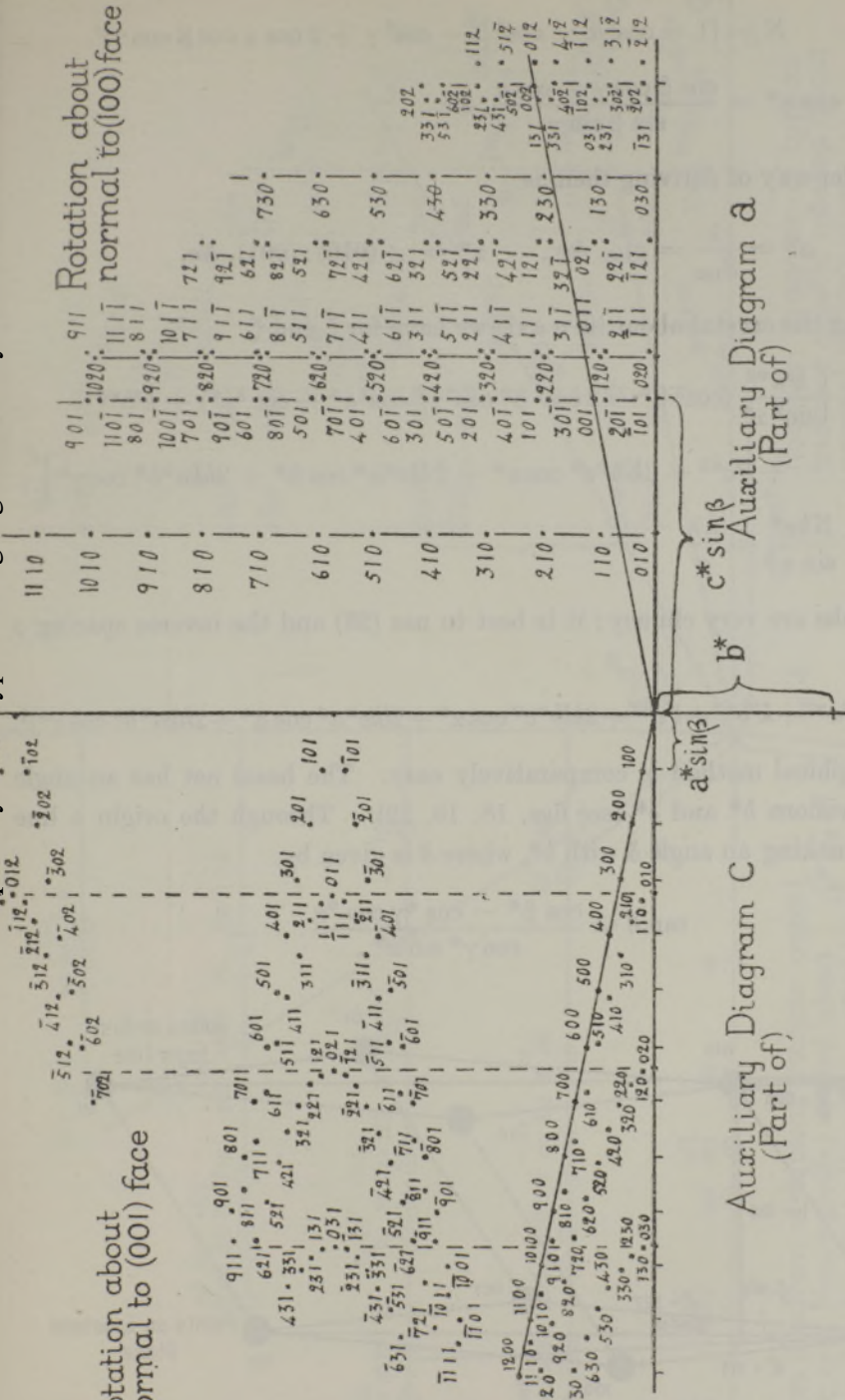


FIG. 17.—Rotation Diagrams of typical Monoclinic Crystal rotated about the normals to the (100) and (001) faces. (See fig. 16.)

where

$$N = \{1 - \cos^2 \alpha - \cos^2 \beta - \cos^2 \gamma + 2 \cos \alpha \cos \beta \cos \gamma\}^{\frac{1}{2}},$$

$$\cos \alpha^* = \frac{\cos \beta \cos \gamma - \cos \alpha}{\sin \beta \sin \gamma}, \text{ &c.}$$

A simpler way of deriving them is

$$a^* = \frac{\lambda}{d_{100}} = \rho_{100}, \text{ &c.}, \quad \alpha^* = \angle (010):(001), \text{ &c.}$$

Rotating the crystal about its  $a$  axis we have for  $\xi$  and  $\zeta$

$$(25) \quad \xi = \left\{ \frac{h^2 a^{*2}}{\sin^2 \alpha^*} (\cos^2 \beta^* - 2 \cos^2 \beta^* \cos^2 \gamma^* \cos^2 \alpha^* + \cos^2 \gamma^*) + k^2 b^{*2} + l^2 c^{*2} + 2 k l b^* c^* \cos \alpha^* + 2 l h c^* \alpha^* \cos \beta^* + 2 h k a^* b^* \cos \gamma^* \right\}^{\frac{1}{2}},$$

$$(26) \quad \zeta = \frac{N h \xi^*}{\sin \alpha^*} = \frac{h \lambda}{a}.$$

The formulæ are very clumsy: it is best to use (26) and the inverse spacing  $\rho$  given by

$$(27) \quad \rho = \{h^2 a^{*2} + k^2 b^{*2} + l^2 c^{*2} + 2 k l b^* c^* \cos \alpha^* + 2 l h c^* \alpha^* \cos \beta^* + 2 h k a^* b^* \cos \gamma^*\}^{\frac{1}{2}}.$$

The graphical method is comparatively easy. The basal net has an angle  $\alpha^*$  and divisions  $b^*$  and  $c^*$  (see figs. 18, 19, 22). Through the origin a line is drawn making an angle  $\delta$  with  $b^*$ , where  $\delta$  is given by

$$\tan \delta = \frac{\cos \beta^* - \cos \gamma^* \cos \alpha^*}{\cos \gamma^* \sin \alpha^*}.$$

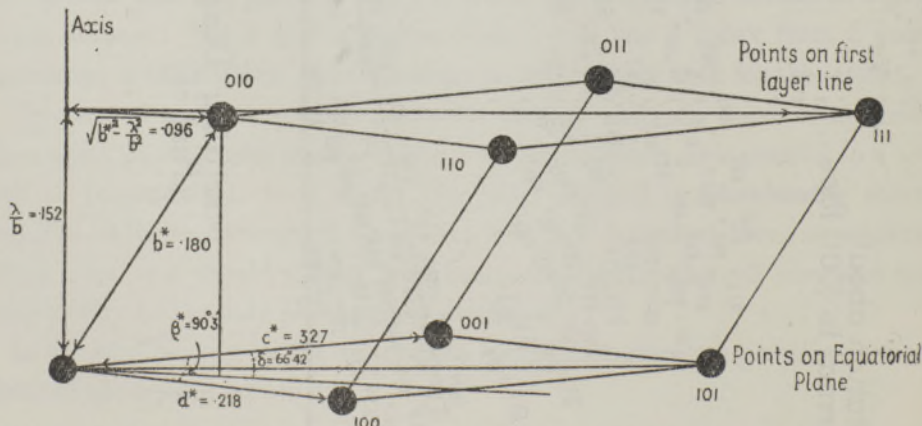
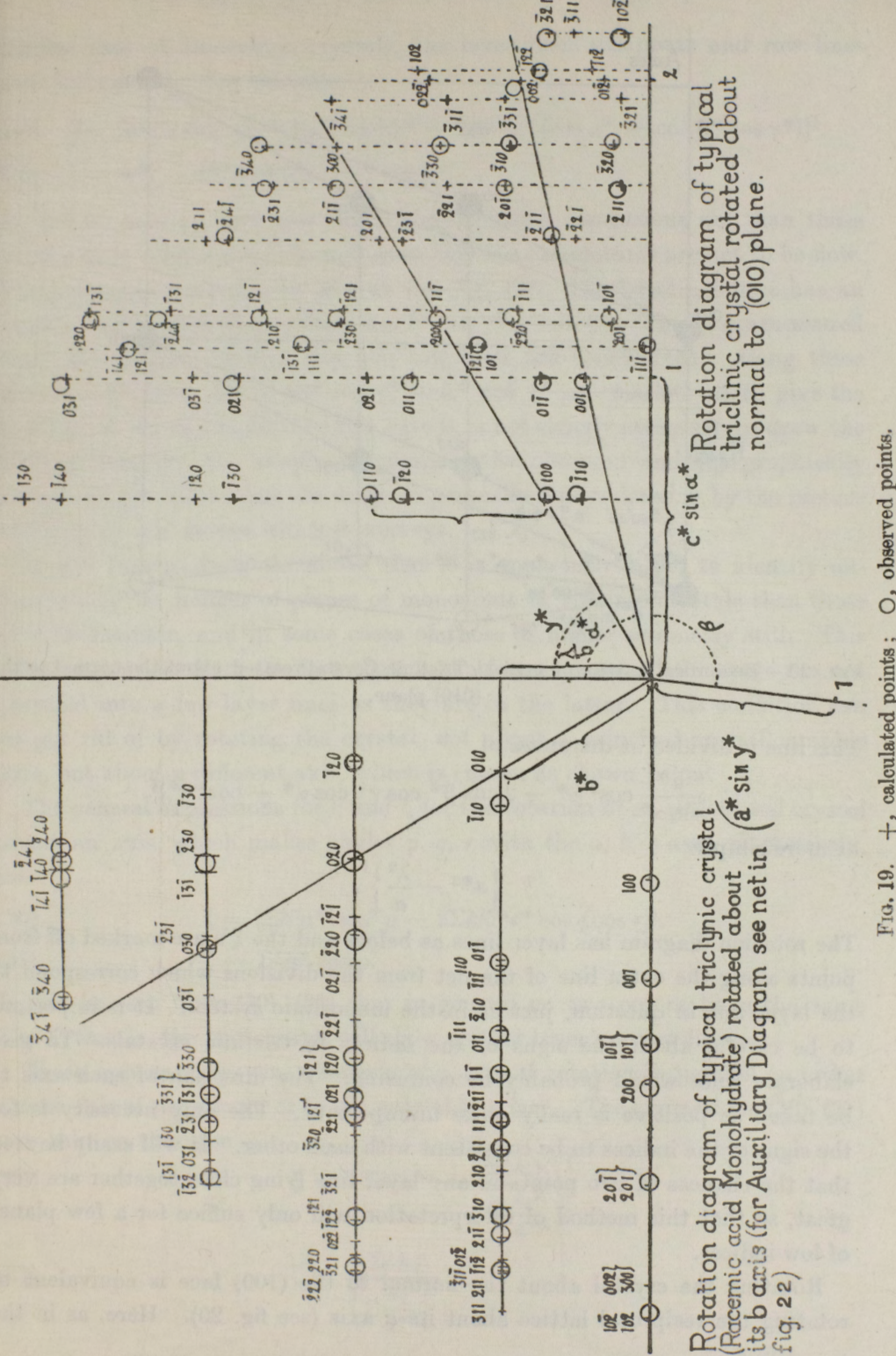


FIG. 18.—Reciprocal Lattice of typical Triclinic Crystal (Racemic Acid Monohydrate) rotated about its  $b$  axis.



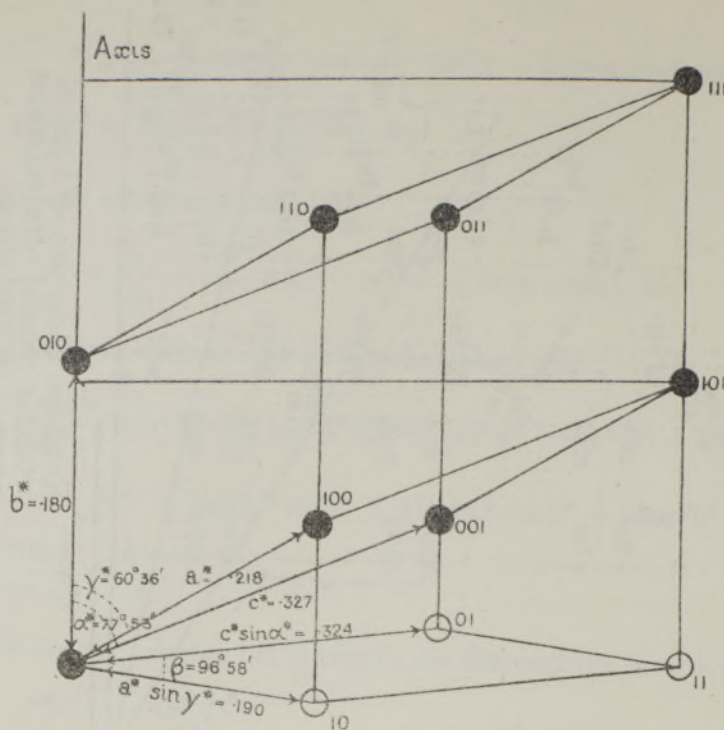


FIG. 20.—Reciprocal Lattice of typical Triclinic Crystal rotated about the normal to the (010) plane.

This line is divided at distances of

$$\frac{a^*}{\sin \alpha^*} \cos^2 \beta^* - 2 \cos \beta^* \cos \gamma^* \cos \alpha^* + \cos^2 \gamma^* }{ }^{\frac{1}{2}},$$

or more simply

$$\left\{ a^{*2} - \frac{\lambda^2}{a} \right\}^{\frac{1}{2}}.$$

The rotation diagram has layer lines as before and the  $\xi$ 's are marked off from points along the extra line of the net from the divisions which correspond to the layer line in question, just as in the monoclinic system. It is important to be careful about the signs of the indices in triclinic crystals. To give elaborate rules would probably be confusing. The direction of each axis to be taken as positive is really quite unimportant. The only necessity is for the signs of the indices to be consistent with each other. It will easily be seen that the chances of two points in any layer line lying close together are very great, so that this method of interpretation will only suffice for a few planes of low indices.

Rotating the crystal about the normal to the (100) face is equivalent to rotating the reciprocal lattice about its  $a$  axis (see fig. 20). Here, as in the

similar case of monoclinic crystals, the layer lines disappear and row lines take their place. For this case

$$(28) \quad \xi = \{k^2 b^{*2} \sin^2 \gamma^* + l^2 c^{*2} \sin^2 \beta^* + 2klb^*c^* (\cos \alpha^* - \cos \beta^* \cos \gamma^*)\}^{\frac{1}{2}},$$

$$(29) \quad \zeta = ha^* + kb^* \cos \gamma^* + lc^* \cos \beta^*.$$

It will be seen at once how much simpler these expressions are than those for the zone axial setting, though even here the calculations are apt to be slow. The graphical method is as follows (see fig. 19). The basal net here has an angle  $\alpha$ , *not*  $\alpha^*$ , and the divisions are  $b^* \sin \gamma^*$ ,  $c^* \sin \beta^*$ . The  $\xi$ 's are measured from the origin. In this way the row lines are constructed. Along these lines the distances  $ha^* + kb^* \cos \gamma^* + lc^* \cos \beta^*$  are marked off to give the position of the points  $hkl$ . In this case it is not strictly necessary to draw the rotation diagram, but simply to compare the observed and the graphically obtained  $\xi$ 's and  $\zeta$ 's; but the diagram generally repays drawing by the picture of the reciprocal lattice which it conveys.

It will be seen from the above that it is apparently easier to identify unequivocally the indices of planes of monoclinic or triclinic crystals than those of orthorhombic, and in some cases of those of higher symmetry still. This advantage arises from the fact that in the former cases all the spots are not crowded into a few layer lines as they are in the latter. This condition can be got rid of by rotating the crystal, not about a principal crystallographic axis, but about a different axis, which is chosen as shown below.

The general expressions for  $\xi$  and  $\zeta$  for the rotation of an orthogonal crystal about an axis, which makes angles  $p$ ,  $q$ ,  $r$  with the  $a$ ,  $b$ ,  $c$  axes respectively, are

$$(30) \quad \xi = \{\sum h^2 a^{*2} \sin^2 p - 2\sum k l b^* c^* \cos q \cos r\}^{\frac{1}{2}},$$

$$(31) \quad \zeta = \sum h a^* \cos p.$$

It can be seen from (30), (31) that in general no two points have the same  $\xi$  or  $\zeta$ , that is, the photograph will show neither layer nor row lines.

These appear, however, whenever the axis of rotation is parallel to either a zone axis of the crystal or to the normal to a face. The expressions (30), (31) now take on the form

$$(32) \quad \xi = \left\{ \sum h^2 a^{*2} - \frac{(\sum h h_z)^2}{\sum \frac{h_z^2}{a^{*2}}} \right\}^{\frac{1}{2}},$$

$$(33) \quad \zeta = \frac{\sum h h_2}{\left\{ \sum \frac{h_2^2}{a^{*2}} \right\}^{\frac{1}{2}}},$$

where  $[h_2 k_2 l_2]$  is a zone axis of the crystal, or

$$(34) \quad \xi = \left\{ \frac{\sum b^{*2} c^{*2} k_p^2 l_p^2 \left( \frac{k}{k_p} - \frac{l}{l_p} \right)^2}{\sum h_p^2 a^{*2}} \right\}^{\frac{1}{2}},$$

$$(35) \quad \zeta = \frac{\sum h_p a^{*2}}{\{\sum h_p^2 a^{*2}\}^{\frac{1}{2}}},$$

where  $(h_p k_p l_p)$  is a plane of the crystal.

From (32), (33) it appears that all planes whose indices satisfy

$$hh_z + kk_z + ll_z = n$$

lie on the  $n$ th of the layer lines, whose distance apart is given by  $\lambda/\tau$ , where  $\tau$  is the primitive translation in the direction of the axis

$$(36) \quad \tau = (h_z^2 a^2 + k_z^2 b^2 + l_z^2 c^2)^{\frac{1}{2}} = \lambda \left( \frac{h_z^2}{a^{*2}} + \frac{k_z^2}{b^{*2}} + \frac{l_z^2}{c^{*2}} \right)^{\frac{1}{2}}.$$

There are in general no row lines. Row lines appear when any two of  $h_z k_z l_z$  vanish together, *i.e.*, when the axis is a principal one; when  $a, b, c$  are commensurable, *i.e.*, in the cubic system; or when  $l_z = 0$  and  $a, b$  are commensurable, *i.e.*, for axes perpendicular to the  $c$  axis in tetragonal, hexagonal and trigonal systems.

From (34), (35) it appears that all planes whose indices satisfy

$$\frac{h - h'}{h_p} = \frac{k - k'}{k_p} = \frac{l - l'}{l_p},$$

where  $h' h_p + k' k_p + l' l_p = 0$ , lie on row lines whose  $\xi$  is given by (34) with  $h' k' l'$  in the place of  $hkl$ , and on these lines the points are separated by the same common distance  $(h_p^2 a^{*2} + k_p^2 b^{*2} + l_p^2 c^{*2})^{\frac{1}{2}}$  inversely proportional to the spacing of the plane perpendicular to which the axis lies. Layer lines do not appear except in the same particular cases as in the last section. Both these modes of setting give rise to photographs that are rather too complicated to interpret rapidly, except, of course, in the cubic system.

If we limit the choice of axes still farther, so that it lies in one of the principal planes of the crystal, say the  $a, b$  plane, we have in general

$$(37) \quad \xi = \{l^2 c^{*2} + (ha^* \sin p - kb^* \cos p)^2\}^{\frac{1}{2}},$$

$$(38) \quad \zeta = ha^* \cos p + kb^* \sin p.$$

Now, if we choose  $p$  very small, that is, if the axis of rotation is very near the  $a$  axis, (37), (38) take the form

$$(39) \quad \xi \doteq \{k^2b^{*2} + l^2c^{*2}\}^{\frac{1}{2}} - \frac{hka^*b^*p}{\{k^2b^{*2} + l^2c^{*2}\}^{\frac{1}{2}}},$$

$$(40) \quad \zeta \doteq ha^* + kb^*p.$$

Spots lying on a layer line on the photograph about the  $a$  axis will now lie on a series of very close layer lines separated by a distance  $b^*p$ , so that unless  $l$  is very large  $h$  and  $k$  may be read off directly from (40) and thus furnish a way of separating the spots corresponding to the two planes  $(hkl)$  and  $(h'k'l')$  for which  $k^2b^{*2} + l^2c^{*2} \doteq k'^2b^{*2} + l'^2c^{*2}$ . The smaller  $p$ , the more such points approach each other; the larger  $p$ , on the other hand, the more chance that  $ha^* + kb^*p$  be confused with  $h'a^* + k'b^*p$ .  $p$  should therefore be chosen so that  $b^*p$  is just outside the limit of resolution of  $\zeta$ .

The theoretical rotation diagram is constructed as follows:—An ordinary diagram is drawn with layer lines  $a^*$  apart; parallel to these and on each side of them are drawn six or seven layer lines at a distance apart of  $b^*p$ . The  $\xi$  axis is divided, as before, at points corresponding to the planes  $(0kl)$ , and from each of these is drawn two lines at a gradient of  $\pm kb^*p/\zeta_{kl}$ . Where these lines meet the layer lines  $ha^* \mp kb^*p$  respectively are the positions corresponding to the planes  $(hkl)$ ,  $(h\bar{k}l)$ . This construction becomes too inaccurate to be used when  $p > 3^\circ$ . A construction available for all angles is to draw the layer lines as before but with the distance  $b \sin p$  between the subsidiary ones, but instead of drawing row lines to cut off along the corresponding layer lines distances from the centre

$$(41) \quad \varphi = \{h^2a^{*2} + k^2b^{*2} + l^2c^{*2}\}^{\frac{1}{2}}.$$

The appearance of the rotation diagram taken with this form of setting is shown in fig. 12. Each spot in the axial photograph is split into two  $(hkl)$  and  $(h\bar{k}l)$ , recognisable by their spacing as belonging to the same form. Their vertical separation gives at once the  $c$  index. If there are two spots of nearly the same spacing, they must separate to different degrees and become in consequence distinguishable.

If the axis of rotation is taken along the zone axis  $[h_z k_z 0]$ , (37), (38) take the form

$$(42) \quad \xi = \left\{ l^2c^{*2} + \frac{(hk_z a^{*2} - h_z k b^{*2})^2}{k_z^2 a^{*2} + h_z^2 b^{*2}} \right\}^{\frac{1}{2}},$$

$$(43) \quad \zeta = \frac{a^*b^*(hh_z + kk_z)}{\{k_z^2 a^{*2} + h_z^2 b^{*2}\}^{\frac{1}{2}}}.$$

This case is completely analogous to that of a monoclinic crystal rotated about its *a* or *c* axis. It shows layer lines, but row lines only if *a* and *b* are commensurable, that is, in the cubic, tetragonal, hexagonal and trigonal systems. The rotation diagram is best constructed as in the monoclinic system. The zone axis chosen depends, of course, on the habit of the crystal, but it must be remembered that if the purpose of the photograph is to separate planes of nearly equal spacing, the axis must have high indices, and for the photograph to be easily interpretable it must lie fairly close to a crystallographic axis so that it will not in general be represented by a zone of faces in the crystal, and its position will have to be calculated.

For the purpose of separating planes the method of setting with the axis perpendicular to a plane is to be preferred. If the indices of the plane are  $(h_p k_p 0)$  we have

$$(44) \quad \xi = \left\{ l^2 c^{*2} + \frac{a^{*2} b^{*2} (hk_p - h_p k)^2}{h_p^2 a^{*2} + k_p^2 b^{*2}} \right\}^{\frac{1}{2}},$$

$$(45) \quad \zeta = \frac{hh_p a^* + kk_p b^*}{\{h_p^2 a^{*2} + k_p^2 b^{*2}\}^{\frac{1}{2}}}.$$

This method is analogous to the setting of a monoclinic crystal with the axis perpendicular to (100) or (001). It shows row lines, but layer lines only in the special cases of the last section, where the two methods become identical. The rotation diagram is constructed as in the monoclinic system, except in these special cases where the construction is that of the orthorhombic system. In contradistinction to the previous case, the choice of indices need not be high in order to get resolution.

Even by the methods just dealt with it is often impossible to be sufficiently sure of the indices of the spots, and at the same time to be sure that the reflections of all possible planes have been noticed. Both these disadvantages are overcome in the oscillation method. The method takes more time, but as it increases the intensity of the spots proportionately, this is rather an advantage.

In all the methods of interpretation of rotation photographs suggested heretofore we have only used two measured quantities, the co-ordinates of the spot on the plate, to determine the three indices of a plane, and have made use of the integral nature of these indices to see which of them satisfied the observations. It has been seen that this leads to ambiguities. Two or more planes may give reflections at almost the same place on the plate, and the best resolving power we can obtain may be insufficient to separate them. It is obvious that if we could tell precisely at what angular position of the crystal

any given plane reflects, we would be provided with a third independent measured quantity and could determine the indices of the plane unequivocally without even making use of their integral nature. Unfortunately to do this would involve the use of a fluorescent screen capable of showing reflections from all crystal planes, and nothing even approaching such sensitivity has yet been produced. It is, however, possible to approximate to these conditions with photographic methods, and to do so as closely as we like if we are prepared to take sufficient pains. The crystal, mounted as in the rotation method, is turned about an axis perpendicular to the X-ray beam, not through a whole revolution but through some definite angle. (In practice it is oscillated backwards and forwards through this angle, hence the name "Oscillation Method.") Then the spots which appear on the photograph are due to those planes, and those planes alone, whose reflecting positions lie within that angle. If the range of oscillation, as this angle is called, be made small enough, the photograph will contain no spots of ambiguous indices.

As we have seen on p. 122, the points of the reciprocal lattice which give reflections for any given direction of incident rays lie on a sphere, which has the incident ray for diameter, which passes through the origin and whose radius is  $k^2/\lambda = 1$ . If we consider the direction of the rays to rotate through an angle  $\eta$ , the points which reflect lie inside the volume swept out by the surface of the sphere of reflection. This volume is divided into two parts. If we consider the sphere to be divided into two hemispheres by a plane passing through the axis of rotation, then the points of the reciprocal lattice which intersect the one hemisphere give reflections on one side of the principal plane and those intersecting the other hemisphere on the other side. The volume swept out is therefore divided into two interpenetrating volumes each representing that swept out by a hemisphere and thus planes which reflect on one side or the other of the principal plane. The common part of the volume corresponds to planes reflecting on both sides of the principal plane and the toroidal surface swept out by the sphere corresponds to points giving reflections in the principal plane itself. From this we can see that the existence of a reflection on one side or the other of the principal plane which occurs during a rotation of the crystal through a finite angle shows that the corresponding point in the reciprocal lattice lies inside the volume swept out by a hemisphere rotated through that angle about a tangent to its diametral circle. The smaller the angle the more limited the choice of points lying in this volume and the more certain the identification of the indices of the plane responsible for the reflection.

Consider a plane whose co-ordinates referred to the reciprocal lattice are  $\xi, \zeta, \omega$ ,  $\omega$  being measured from some initial line fixed in the crystal (see fig. 5). Let  $\eta$  be the angle between the direction of the incident ray and the initial line. Then the condition that a given plane reflects is

$$(46) \quad \cos(\omega - \eta) = \frac{\xi^2 + \zeta^2}{2\xi},$$

with the further condition that the reflection takes place to the right or left of the principal plane according as  $(\omega - \eta)$  is positive or negative respectively.

In an oscillation photograph we know  $\xi, \zeta$  from the position of the spot on the plate and  $\eta$  we know to lie between two limiting values  $\eta_1, \eta_2$ . We therefore have to determine  $\omega$  the inequality

$$(47) \quad \eta_1 + \cos^{-1} \frac{\xi^2 + \zeta^2}{2\xi} < \omega < \eta_2 + \cos^{-1} \frac{\xi^2 + \zeta^2}{2\xi},$$

the signs of  $\cos^{-1} \frac{\xi^2 + \zeta^2}{2\xi}$  being determined by the second condition.

Now the problem for which the oscillation method was introduced is that of finding the indices of spots whose  $\xi, \zeta$  co-ordinates are not sufficiently distinguishable from each other. If we know the crystal and the way it is set up, including the direction of the initial line, we can calculate the  $\omega$  co-ordinates  $\omega_1, \omega_2, \omega_3 \dots \omega_n$  of the planes  $h_1 k_1 l_1, h_2 k_2 l_2, h_3 k_3 l_3 \dots h_n k_n l_n$ , whose  $\xi, \zeta$  co-ordinates  $\xi_1 \zeta_1, \xi_2 \zeta_2, \xi_3 \zeta_3 \dots \xi_n \zeta_n$  all lie between  $\xi + \delta\xi, \xi - \delta\xi; \zeta + \delta\zeta, \zeta - \delta\zeta$  respectively, where  $\delta\xi, \delta\zeta$  represent the limits of error of  $\xi, \zeta$  depending on resolving power and accuracy of the apparatus. Of these  $\omega$ 's only one  $\omega_r$  may satisfy the inequality (47); the reflecting plane is then unequivocally  $h_r k_r l_r$ . On the other hand, two or more may satisfy the inequality so that the indices still remain in doubt, but in any case several possible sets of indices will be eliminated. To determine the indices in such doubtful cases we must either narrow the range of oscillation by diminishing  $(\eta_2 - \eta_1)$ , or we must change the rotation axis, or both.

The procedure in taking oscillation photographs only differs from that in rotation photographs by the fact that the axial angular position of the crystal with respect to the incident ray becomes important. For oscillation photographs, therefore, the head is fitted with an index reading on a fixed circle, so that if the angular position of the crystal is known for one position it can be found for all. The crystal is set up for oscillation photographs precisely as for ordinary rotation photographs. In most cases a prominent zone axis

is chosen as axis of rotation, but the axis may be chosen to be perpendicular to some prominent plane. In the first case one of the planes of the zone is chosen as reference plane, *i.e.*, its normal is the initial line. For simplicity of calculation it is best to choose a pinacoid face. This plane has now to be brought as nearly as possible perpendicular to the incident beam ; how this is to be done depends upon the apparatus. From this initial position we take successive oscillations through angles of  $5^\circ$ ,  $10^\circ$ , or  $15^\circ$  until  $90^\circ$  or  $180^\circ$  have been turned through according to the symmetry of the crystal. If the oscillation photograph is required to give intensity measurements, it is necessary to cover the ground twice with overlapping photographs.

The interpretation of oscillation photographs is simply an extension of that of rotation photographs. As before, we determine the  $\xi$ ,  $\zeta$  co-ordinates of each spot and compare them with the theoretical  $\xi$ ,  $\zeta$ 's either numerically or graphically. At this stage we can employ two methods : we may determine by means of the criterion (47) whether one or more than one point of nearly the same  $\xi$ ,  $\zeta$  will give a reflection in the range of oscillation and do this for every value of  $\xi$ ,  $\zeta$  ; or we may determine beforehand the  $\xi$ ,  $\zeta$ 's of all the planes which reflect within the range of the oscillation and restrict ourselves to these planes in determining the indices corresponding to the observed values of  $\xi$ ,  $\zeta$ . Except where it is a question of resolving a very few particular spots, the first method is much too laborious to be of any use in practice.

The second method is best carried out graphically. Now the occurrence of a reflection may be regarded as the intersection of the sphere of reflection with a point of the reciprocal lattice. If consequently we project this three-dimensional scheme normally on to the equatorial plane, we get a reflection whenever a point in the projection of the reciprocal lattice intersects the projection of the circle of section of the sphere of reflection by a plane through the point parallel to the equatorial plane (see fig. 3 and fig. 21). We have therefore simply to rotate such circles about the pole of the axis through the angle of oscillation and mark the indices of the points which during the oscillation intersect their corresponding circles. The operations are greatly simplified if, as in rotation photographs, we take as axis a zone axis of the crystal, for here the points of the reciprocal lattice lie in planes parallel to the equatorial plane, and instead of there being in general a circle of section corresponding to each spot on the plate, there is only one corresponding to each layer line. At the same time the disadvantages which this method of setting offers in rotation photographs on account of lack of resolving power do not exist in the oscillation method.

We will first consider the case where the axis of rotation is a primitive vector of the reciprocal lattice as in all orthogonal crystals about their principal axes and monoclinic crystals about the  $b$  axis. Here the projection of the reciprocal lattice on the equatorial plane is simply the net of points in that plane, as each point in any parallel net projects into the corresponding point in the equatorial plane net, *i.e.*, the point  $hkl$  projects on to the point  $0kl$  if  $a$  is the

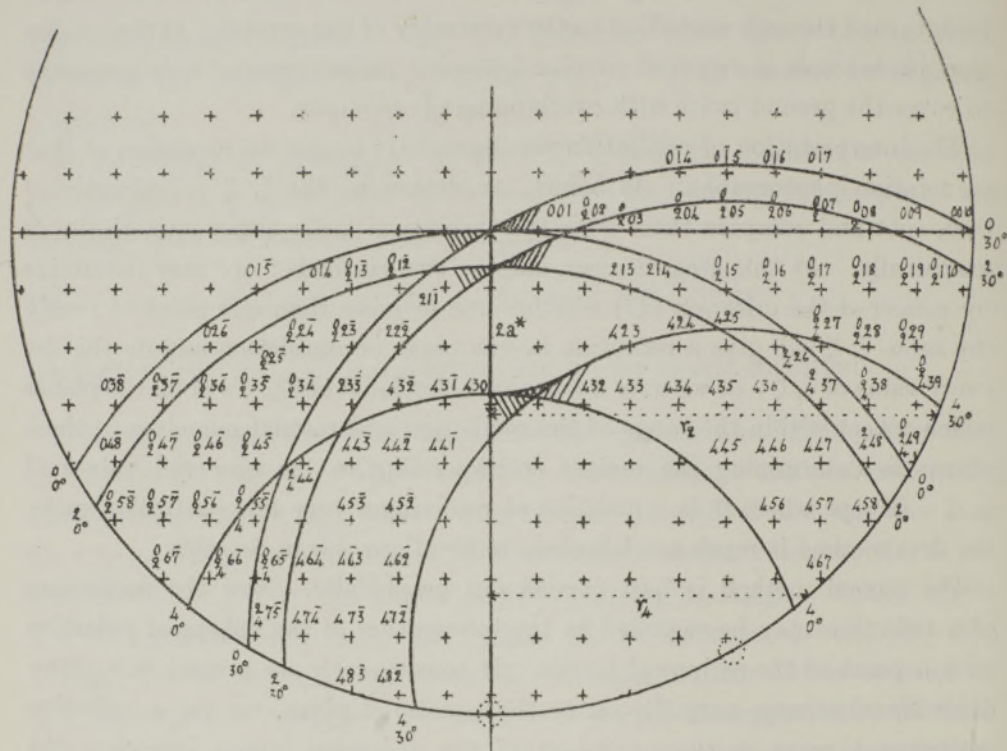


FIG. 21.—Oscillation Diagram for typical Orthorhombic Crystal ( $\beta$ -form of Gallium Acetylacetone) for a  $30^\circ$  Oscillation about the  $a$  Axis. Only the Equatorial, 2nd and 4th Circles of Section shown.

$\pm$ , Point of the  $b^* c^*$  net.       $////$ , Reflection to right.       $\backslash\backslash\backslash\backslash$ , Reflection to left.  
 $\frac{2}{4}44$ , Indices of points appearing in the oscillation on 2nd and 4th layer line of 2nd and  
 4th circles.

axis of rotation. Further, all the points  $hkl$ , where  $h$  is constant, have as their corresponding circle of section that cut from the sphere of reflection by a plane  $ha^*$  from the equatorial plane. The actual construction can best be done as follows (see fig. 21):—The basal net is drawn as before, the amount of it to be included depending on the dimensions of the apparatus. A circle of

unit radius is drawn about the origin, and on its circumference are marked off points whose angular positions correspond to the limits of the different oscillations. These are the centres of the circles of section. The radii of the latter are obtained from the same diagram by marking off distances  $a^*2a^*$ , ..., along  $d$  and drawing parallel to  $c$  straight lines meeting the circle of centres. These lines are the radii of the first, second, etc., ... circles of section, that of the zero circle of section being, of course, unity. Circles of these radii are drawn about each of the centres. Then if, in the two lunular spaces, between the two  $h$ th circles about neighbouring centres there occur the points  $k_1l_1$ ,  $k_2l_2$ , ..., in the basal net, the planes  $(hk_1l_1)$   $(hk_2l_2)$ , ..., reflect in the oscillation in question. Those in one lune reflect to the right; those in the other to the left. Lists of planes are made and compared with those occurring on the plates for the corresponding oscillations, the values of  $\xi$  being used as a check. It should be remembered, however, that the imperfections of the crystals and the divergence of the beam limit the accuracy of the method, so that every oscillation will be found to contain spots belonging to a region of  $2^\circ$  or so on each side of it, or more if the crystal is markedly imperfect.

In triclinic crystals and monoclinic crystals rotated about their  $a$  or  $c$  axes, the points on successive layers do not project normally on to each other in the equatorial plane. On the projection the nets representing successive layers are displaced through a distance  $a^* \cos \beta$  in the  $c^*$  direction in the monoclinic system and

$$\frac{a^*}{\sin \alpha^*} (\cos^2 \beta^* - 2 \cos \beta^* \cos \gamma^* \cos \alpha^* + \cos^2 \gamma^*)^{\frac{1}{2}} \quad \text{or} \quad \left\{ a^{*2} - \frac{\lambda^2}{a^2} \right\}^{\frac{1}{2}}$$

in a direction, making an angle  $\delta$  with  $b^*$  where

$$\tan \delta = \frac{\cos \beta^* - \cos \gamma^* \cos \alpha^*}{\cos \gamma^* \sin \alpha^*}$$

in the triclinic system. We could draw this projection and proceed as before, but a simpler plan is to move the circle of centres for each layer by the same amount in the opposite direction (see fig. 22).

An alternative method is to use the basal net, drawn on a piece of tracing-paper, in conjunction with a set of circles of section, and rotate it about its origin in the case of orthogonal crystals, and in the case of monoclinic and triclinic crystals about successively displaced centres.

It may be necessary, though it is rarely advisable, to take oscillation photographs with the normal to a face as rotation axis. In this case all the spots

in the reciprocal lattice project on to the equatorial net, but here in general there are no layer lines, so that each point has its own particular circle of section.

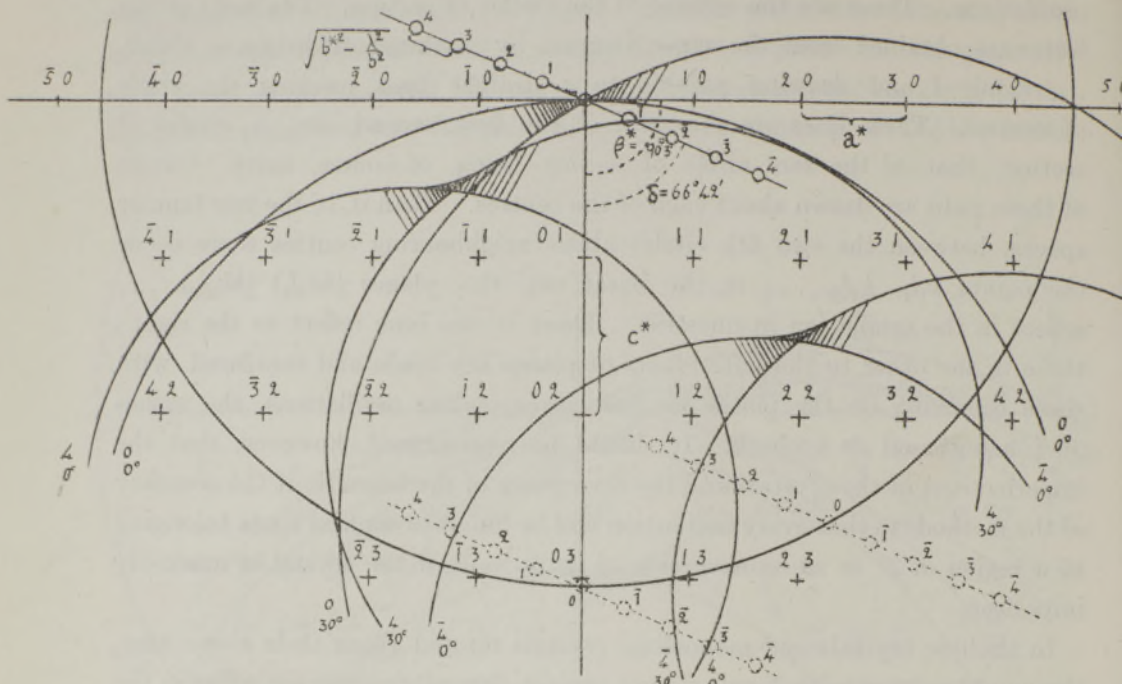


FIG. 22.—Oscillation Diagram and Auxiliary Diagram combined for typical Triclinic Crystal for a rotation about the  $b$  axis from 0 to  $30^\circ$  from the normal to the (001) plane.

+, Point of  $c^*a^*$  net.

○, Points for Auxiliary Diagonal of fig. 19.

It would be much too laborious to draw all these circles, but we can make use of a set of circles drawn for ascending values of  $\zeta$  (Chart 4). By interpolation from these we can find at what position of the crystal a point will cut a circle of corresponding  $\zeta$ . This chart may be used conveniently for all oscillation photographs. Here it is easier to find the angles of reflection for each plane than to find the indices of those planes which reflect within a given angle of oscillation.

When by any of the above methods the indices of all the reflecting planes have been observed, it is of the greatest importance to pay particular attention to absent planes. It is not sufficient to make a list of indices up to certain values and mark as absent those that do not appear on any plate. We must first be certain that these planes have been in a reflecting position, and if not additional photographs must be taken. Absent planes should be looked for in their expected places individually. From lists of reflections checked in

this way the space group can usually be found by referring to the tables of Astbury and Yardley, or to those of Wyckoff.

We have now completed in a summary manner the account of the methods used to measure the cell of a crystal and the indices of its reflecting planes. These methods have all been tested in practice and it has been found that even for complex organic crystals, some of which give over 500 measurable planes, they are sufficient in themselves to do this. References would be given, but so far none of the work has had time to be published.\* It is not suggested, however, that the rotation method should ever be used alone in crystal analysis. To make the best use of the data it gives, it needs to be supplemented by the Ionisation Spectrometer and Laue methods. Its particular value lies in its power to determine unequivocally the true cell size, a point which both the other methods are liable to mistake. Besides this, it gives information as to reflections from a great number of planes, particularly general planes which would be tedious or impossible to find by the Ionisation Spectrometer. The Laue method certainly gives more reflections, but these have not the same value, because their intensities depend on so many more factors than in the rotation method. The question of intensity measurements in rotation photographs cannot be gone into here. It is sufficient to say that several methods have been used or are in process of development and that the accuracy of measurement tends to approach though never to equal that of the Ionisation Spectrometer.

The author wishes to thank Sir William Bragg and the workers of the Davy Faraday Laboratory, without whose co-operation the present work would have been impossible, and the Council of the Royal Institution of Great Britain for their financial assistance.

#### *Summary.*

The interpretation of single crystal rotation photographs divides itself into three parts. It is first shown by means of formulæ, tables and charts how the reciprocal lattice cylindrical co-ordinates  $\xi$ ,  $\zeta$  can be found for each spot on the photographs. In the second part it is shown how to arrive at the dimensions of the true cell by means of the positions of the layer lines on the photograph. The third part consists in the attribution of the correct indices to the spots. It is shown by formulæ and graphical equivalents how to derive

\* Astbury, *loc. cit.*

from the dimensions of the cell the  $\xi$ ,  $\zeta$  values of the different planes for various settings of crystals of different symmetry classes, and how, by comparing these with the results of the first part, to find which are the reflecting planes. Finally, several methods, of which the oscillation method is by far the most valuable, are given for the separation of spots whose closeness lead to ambiguities in the normal rotation method.

Tables for Plane Plate.

1 Tan $2\theta$ .	2 $2 \sin \theta$ .	3 Sec $2\theta$ .	4 $\frac{\cos \theta}{\cos 2\theta}$ .	5 Sec $\theta$ .	6 Log sec $2\theta$ .	7 $\log \frac{\cos \theta}{\cos 2\theta}$ .
0.00	0.0000	1.000	1.000	1.0000	0.00000	0.00000
0.01	0.0100	1.000	1.000	1.0000	0.00002	0.00002
0.02	0.0200	1.000	1.000	1.0001	0.00009	0.00007
0.03	0.0300	1.000	1.000	1.0001	0.00020	0.00015
0.04	0.0399	1.001	1.001	1.0002	0.00035	0.00026
0.05	0.0499	1.001	1.001	1.0003	0.00054	0.00041
0.06	0.0599	1.002	1.001	1.0004	0.00078	0.00059
0.07	0.0699	1.002	1.002	1.0006	0.00106	0.00080
0.08	0.0798	1.003	1.002	1.0008	0.00138	0.00104
0.09	0.0897	1.004	1.003	1.0010	0.00175	0.00131
0.10	0.0996	1.005	1.004	1.0013	0.00216	0.00162
0.11	0.1095	1.006	1.004	1.0015	0.00261	0.00196
0.12	0.1194	1.007	1.005	1.0018	0.00310	0.00233
0.13	0.1292	1.008	1.006	1.0021	0.00364	0.00273
0.14	0.1390	1.010	1.007	1.0024	0.00421	0.00316
0.15	0.1488	1.011	1.008	1.0028	0.00483	0.00362
0.16	0.1585	1.013	1.010	1.0032	0.00549	0.00412
0.17	0.1682	1.014	1.011	1.0036	0.00619	0.00465
0.18	0.1779	1.016	1.012	1.0040	0.00692	0.00520
0.19	0.1875	1.018	1.013	1.0044	0.00770	0.00578
0.20	0.1971	1.020	1.015	1.0049	0.00852	0.00640
0.21	0.2066	1.022	1.016	1.0054	0.00937	0.00704
0.22	0.2161	1.024	1.018	1.0059	0.01026	0.00771
0.23	0.2256	1.026	1.020	1.0064	0.01119	0.00841
0.24	0.2350	1.028	1.021	1.0070	0.01216	0.00914
0.25	0.2444	1.031	1.023	1.0075	0.01316	0.00989
0.26	0.2537	1.033	1.025	1.0081	0.01420	0.01068
0.27	0.2629	1.036	1.027	1.0087	0.01528	0.01149
0.28	0.2721	1.039	1.029	1.0094	0.01639	0.01233
0.29	0.2813	1.041	1.031	1.0100	0.01753	0.01320
0.30	0.2904	1.044	1.033	1.0107	0.01871	0.01409
0.31	0.2995	1.047	1.035	1.0114	0.01992	0.01500
0.32	0.3085	1.050	1.037	1.0121	0.02117	0.01594
0.33	0.3174	1.053	1.040	1.0128	0.02245	0.01691
0.34	0.3263	1.056	1.042	1.0136	0.02375	0.01789
0.35	0.3351	1.059	1.044	1.0143	0.02509	0.01890
0.36	0.3438	1.063	1.047	1.0151	0.02646	0.01994
0.37	0.3525	1.066	1.050	1.0159	0.02786	0.02101
0.38	0.3611	1.070	1.052	1.0167	0.02929	0.02210
0.39	0.3697	1.073	1.055	1.0175	0.03075	0.02320

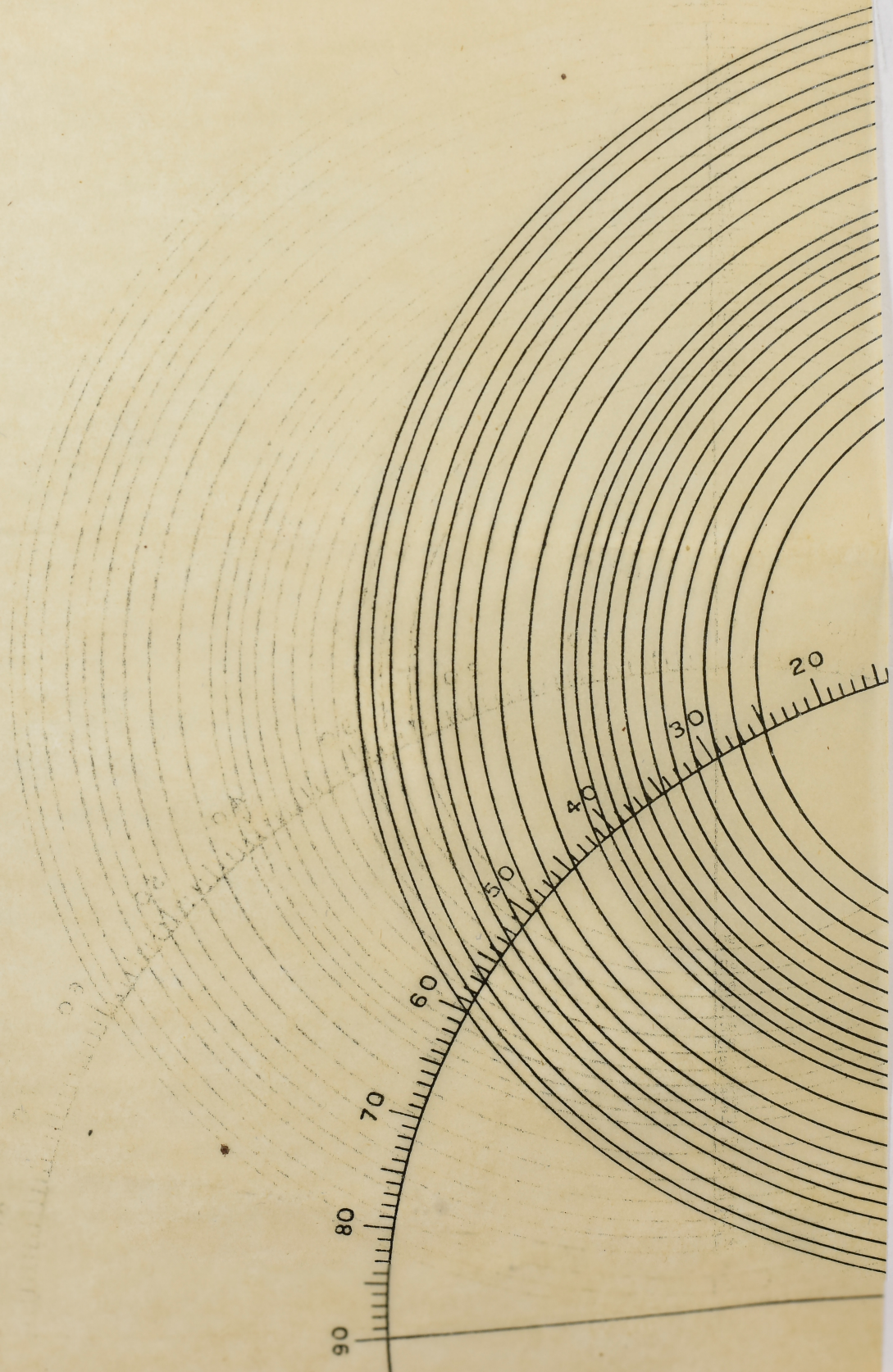


CHART IV.

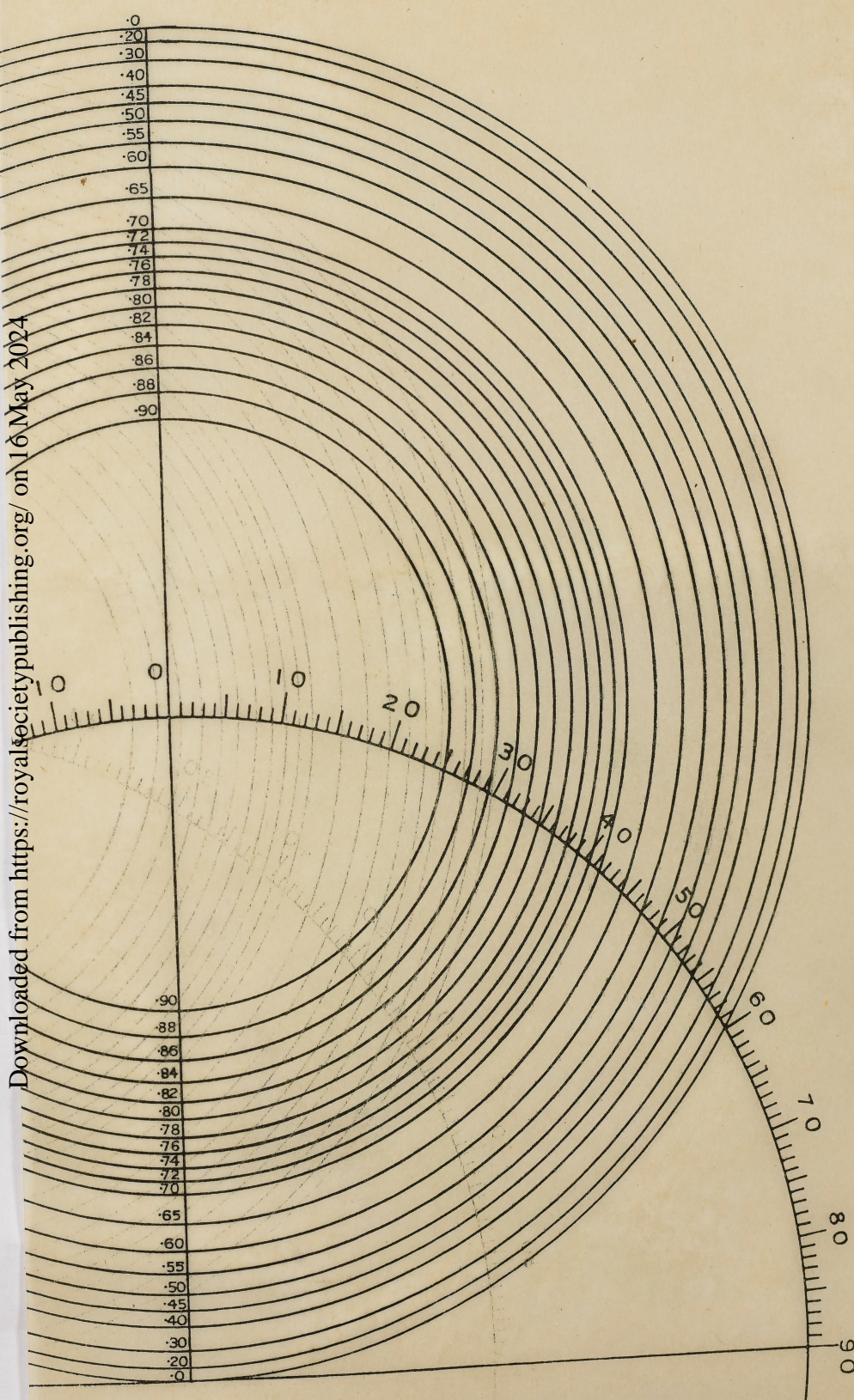


Table for Plane Plate—(continued).

1 Tan $2\theta$ .	2 $2 \sin \theta$ .	3 Sec $2\theta$ .	4 $\frac{\cos \theta}{\cos 2\theta}$ .	5 Sec $\theta$ .	6 Log sec $2\theta$ .	7 $\log \frac{\cos \theta}{\cos 2\theta}$ .
0.40	0.3782	1.077	1.058	1.0184	0.03223	0.02432
0.41	0.3866	1.081	1.060	1.0192	0.03374	0.02547
0.42	0.3950	1.085	1.063	1.0201	0.03528	0.02664
0.43	0.4033	1.089	1.066	1.0210	0.03684	0.02783
0.44	0.4115	1.093	1.069	1.0219	0.03843	0.02903
0.45	0.4197	1.097	1.072	1.0228	0.04004	0.03026
0.46	0.4278	1.101	1.075	1.0237	0.04168	0.03151
0.47	0.4358	1.105	1.078	1.0246	0.04334	0.03278
0.48	0.4438	1.109	1.082	1.0256	0.04502	0.03406
0.49	0.4517	1.114	1.085	1.0266	0.04673	0.03537
0.50	0.4595	1.118	1.088	1.0275	0.04846	0.03669
0.51	0.4673	1.123	1.092	1.0285	0.05020	0.03802
0.52	0.4750	1.127	1.095	1.0295	0.05197	0.03936
0.53	0.4826	1.132	1.098	1.0305	0.05376	0.04072
0.54	0.4901	1.136	1.102	1.0315	0.05557	0.04211
0.55	0.4976	1.141	1.105	1.0325	0.05739	0.04352
0.56	0.5050	1.146	1.109	1.0335	0.05923	0.04493
0.57	0.5123	1.151	1.113	1.0345	0.06109	0.04636
0.58	0.5196	1.156	1.116	1.0355	0.06297	0.04780
0.59	0.5268	1.161	1.120	1.0366	0.06486	0.04925
0.60	0.5339	1.166	1.124	1.0376	0.06677	0.05072
0.61	0.5409	1.171	1.128	1.0387	0.06869	0.05220
0.62	0.5479	1.177	1.132	1.0398	0.07063	0.05369
0.63	0.5548	1.182	1.136	1.0409	0.07258	0.05519
0.64	0.5616	1.187	1.140	1.0419	0.07455	0.05671
0.65	0.5684	1.193	1.144	1.0430	0.07653	0.05824
0.66	0.5751	1.198	1.148	1.0441	0.07852	0.05978
0.67	0.5818	1.204	1.152	1.0452	0.08052	0.06132
0.68	0.5884	1.209	1.156	1.0463	0.08253	0.06287
0.69	0.5949	1.215	1.160	1.0474	0.08456	0.06444
0.70	0.6013	1.221	1.164	1.0485	0.08660	0.06602
0.71	0.6077	1.226	1.168	1.0496	0.08864	0.06760
0.72	0.6140	1.232	1.173	1.0507	0.09069	0.06919
0.73	0.6202	1.238	1.177	1.0519	0.09276	0.07080
0.74	0.6264	1.244	1.181	1.0530	0.09483	0.07241
0.75	0.6325	1.250	1.186	1.0541	0.09691	0.07403
0.76	0.6385	1.256	1.190	1.0552	0.09900	0.07565
0.77	0.6445	1.262	1.195	1.0564	0.10109	0.07728
0.78	0.6504	1.268	1.199	1.0575	0.10320	0.07892
0.79	0.6562	1.274	1.204	1.0586	0.10530	0.08057
0.80	0.6620	1.281	1.208	1.0597	0.10742	0.08222
0.81	0.6677	1.287	1.213	1.0609	0.10954	0.08388
0.82	0.6734	1.293	1.218	1.0620	0.11167	0.08554
0.83	0.6790	1.300	1.222	1.0632	0.11380	0.08721
0.84	0.6845	1.306	1.227	1.0643	0.11594	0.08889
0.85	0.6900	1.312	1.232	1.0654	0.11808	0.09056
0.86	0.6954	1.319	1.237	1.0666	0.12022	0.09224
0.87	0.7008	1.325	1.241	1.0677	0.12237	0.09393
0.88	0.7061	1.332	1.246	1.0688	0.12453	0.09562
0.89	0.7113	1.339	1.251	1.0700	0.12668	0.09731

Table for Plane Plate—(continued).

1 Tan $2\theta$ .	2 $2 \sin \theta$ .	3 Sec $2\theta$ .	4 $\frac{\cos \theta}{\cos 2\theta}$ .	5 Sec $\theta$ .	6 Log sec $2\theta$ .	7 Log $\frac{\cos \theta}{\cos 2\theta}$ .
0.90	0.7165	1.345	1.256	1.0711	0.12884	0.09901
0.91	0.7216	1.352	1.261	1.0722	0.13100	0.10071
0.92	0.7267	1.359	1.266	1.0734	0.13316	0.10241
0.93	0.7317	1.366	1.271	1.0745	0.13533	0.10412
0.94	0.7367	1.372	1.276	1.0756	0.13749	0.10583
0.95	0.7416	1.379	1.281	1.0768	0.13966	0.10754
0.96	0.7465	1.386	1.286	1.0779	0.14183	0.10925
0.97	0.7513	1.393	1.291	1.0790	0.14400	0.11097
0.98	0.7560	1.400	1.296	1.0802	0.14617	0.11269
0.99	0.7607	1.407	1.301	1.0813	0.14834	0.11441
1.00	0.7654	1.414	1.306	1.0824	0.15051	0.11613
1.01	0.7700	1.421	1.312	1.0835	0.15269	0.11785
1.02	0.7745	1.428	1.317	1.0846	0.15486	0.11958
1.03	0.7790	1.436	1.322	1.0858	0.15703	0.12130
1.04	0.7834	1.443	1.328	1.0869	0.15920	0.12302
1.05	0.7878	1.450	1.333	1.0880	0.16137	0.12475
1.06	0.7922	1.457	1.338	1.0891	0.16353	0.12647
1.07	0.7965	1.465	1.343	1.0902	0.16570	0.12820
1.08	0.8007	1.472	1.349	1.0913	0.16787	0.12993
1.09	0.8049	1.479	1.354	1.0924	0.17003	0.13166
1.10	0.8091	1.487	1.360	1.0935	0.17220	0.13339
1.11	0.8132	1.494	1.365	1.0946	0.17436	0.13511
1.12	0.8173	1.501	1.370	1.0957	0.17652	0.13684
1.13	0.8213	1.509	1.376	1.0968	0.17867	0.13856
1.14	0.8253	1.516	1.381	1.0979	0.18083	0.14029
1.15	0.8292	1.524	1.387	1.0989	0.18298	0.14202
1.16	0.8331	1.532	1.392	1.1000	0.18513	0.14374
1.17	0.8370	1.539	1.398	1.1011	0.18727	0.14546
1.18	0.8408	1.547	1.403	1.1021	0.18941	0.14718
1.19	0.8446	1.554	1.409	1.1032	0.19156	0.14891
1.20	0.8483	1.562	1.415	1.1042	0.19369	0.15063
1.21	0.8520	1.570	1.420	1.1053	0.19583	0.15234
1.22	0.8557	1.578	1.426	1.1064	0.19796	0.15406
1.23	0.8593	1.585	1.432	1.1074	0.20008	0.15577
1.24	0.8629	1.593	1.437	1.1085	0.20221	0.15749
1.25	0.8664	1.601	1.443	1.1095	0.20433	0.15920
1.26	0.8699	1.609	1.448	1.1106	0.20645	0.16091
1.27	0.8734	1.616	1.454	1.1116	0.20856	0.16262
1.28	0.8768	1.624	1.460	1.1126	0.21067	0.16433
1.29	0.8802	1.632	1.466	1.1136	0.21278	0.16604
1.30	0.8835	1.640	1.471	1.1147	0.21488	0.16774